Hindawi
Mathematical Problems in Engineering
Volume 2022, Article ID 1330875, 19 pages
https://doi.org/10.1155/2022/1330875

Research Article

Fuzzy Analysis of SVIRS Disease System with Holling Type-II Saturated Incidence Rate and Saturated Treatment

Hu Zhang,[1] V. Madhusudanan,[2] B. S. N. Murthy,[3] M. N. Srinivas,[4] and Biruk Ambachew Adugna[5]

[1]*School of Management Science and Engineering, Anhui University of Finance and Economics, Bengbu 233030, China*
[2]*Department of Mathematics, S.A. Engineering College, Chennai 600077, Tamil Nadu, India*
[3]*Department of Mathematics, Aditya College of Engineering and Technology, Surampalem, Andhra Pradesh, India*
[4]*Department of Mathematics, School of Advanced Sciences, Vellore Institute of Technology, Vellore 632014, Tamil Nadu, India*
[5]*Department of Computer Science, Ambo University, Ambo, Ethiopia*

Correspondence should be addressed to V. Madhusudanan; mvmsmaths@gmail.com and Biruk Ambachew Adugna; biruk.ambachew@ambou.edu.et

Received 1 May 2022; Revised 25 May 2022; Accepted 13 June 2022; Published 29 August 2022

Academic Editor: Punit Gupta

This article presents a fuzzy SVIRS disease system with Holling type-II saturated incidence rate and saturated treatment, in which all parameters related to population dynamics have been considered as fuzzy numbers. Then, the existence condition and permanence of the SVIRS model have been discussed and we derived disease-free and endemic equilibrium points of the proposed fuzzy system. The local stability conditions of the fuzzy system around these equilibrium points using Routh–Hurwitz criteria are discussed. We also verified global stability around the interior steady state using Lozinskii measure. Computer simulations are provided to understand the dynamics of the proposed system. Parameter analysis is carried out with the help of computer simulation. Fuzzy provides better solution for any disease modeling in many ways like disease detection and transmission, different stages of disease, risk analysis (through parameter analysis), and optimal recovery solutions. Earlier literature acts as background to startup this disease modeling and optimal solutions provided by fuzzy logic is one of the motivational key element behind this fuzzy SVIRS model with Holling type-II and its analysis by both analytical and computer simulation.

1. Introduction

Epidemiology, which studies the stealing and determinants of contamination hazard in individual communities, is sometimes referred to as the nucleus discipline of community wellbeing. Mathematical epidemic models aid in the understanding of infectious disease transmission and spread, the recognition of factors leading the transmission procedure in order to discover flourishing organize tactics, and the evaluation of observation strategies and interference procedures. Kermack and McKendrick [1] systematically introduced deterministic models for communicable diseases. In their concept, three epidemiological classes are regarded the fundamental aspects describing infectious diseases [2]: the vulnerable group $S(t)$, the infective class $I(t)$ [3], and the recovered class $R(t)$ [4]. In order to better recognize the process of communicable disease transmission [5], some authors have investigated several types of epidemic systems by taking into account dissimilar compartment models such as SI [6], SIS [7], SIR [8], SIRS [9], SEIR [10], SVEIR [11], and others [12].

In recent years, controlling infectious diseases has become a more difficult task [13]. Vaccination is one approach for controlling infectious diseases [14]. Vaccination is an important component of health treatments aiming at avoiding the spread of transferable diseases because of its wellbeing and rate efficiency [15]. Certainly, high vaccination rates have resulted in dramatic reductions or even eradication of various vaccine-preventable transferable diseases, as seen in the case of smallpox [16]. Nonetheless, one of the most important aspects of vaccination is its level of safety, both in terms of its capacity to prevent sickness and

the longevity of the generated immunity. Some vaccines, such as measles [17], are quite successful, whereas others, such as varicella, are not [18]. Due to medical circumstances, as well as the variation and progress of communicable diseases, the efficacy and levels of fortification offered by a vaccine may gradually reduce with time since the flu virus [19] can evolve quickly. Last year's influenza vaccine is improbable to protect people from this year's viral strains. The measles syndrome [20], which is protected by the measles-mumps-rubella vaccine, does not change substantially from time to time, representative that it is just as probable to defend people now as it was 10 years ago. A quantity of vaccines reduces the risk of infection [21], but they do not prevent the disease from forming and spreading in someone who has been vaccinated [22]. Although these flawed vaccines may not completely avoid contagion [23], they may reduce the likelihood of infection or the severity of infection, hence reducing the burden of infectious disease [24]. Many researchers in the mathematical epidemiology literature have looked at epidemic models with poor immunization [25].

The incidence rate plays an imperative function in determining the dynamics of epidemic models in mathematical modeling of communicable diseases. Kermack and Mckendrick proposed the prevalence rate in its traditional mass action version in 1927. The interaction term in this incidence rate is a linearly rising function of the numeral of infective, which is not optimal for large inhabitants. Anupama et al. [26] postulated a nonlinear prevalence rate for various psychological impacts as a result of this. Anupama et al. were motivated by behavioural changes: during periods of high frequency the apparent threat of disease might become quite high, leading to drastic changes in people's behaviour and, as a result, lowering the real risk of infection. Only a few authors have emphasised the importance of nonlinear frequency rates in the study of infectious disease spread dynamics [27]: Anderson and May [28], Wei and Chen [29], Zhang et al. [30], Li et al. [31], Kumar [32, 33], and Goel [34, 35]. A nonlinear incidence rate SIR model was proposed by Zhou and Fan [36]. At this frequency rate, the quantity of effective interactions between infective and susceptible individuals may oversupply due to an overpopulation of infective individuals. Despite the fact that the dynamics of SIR or SIS diseases models with the saturated incidence rate have been extensively studied in the literature [37], few investigations on the saturated treatment function, even in SEIR epidemic models, have been published [38]. In this article, we will investigate the SEIR model with the saturated incidence rate and saturated treatment function in order to better understand the effects of these points on the spread of infectious diseases [39]. We believe that virus-infected hosts are unable to infect other hosts during the incubation period, and that recovered people and vaccinated-treated people have established eternal resistance and are no longer susceptible to infection [36].

In recent literature, disease models with fuzzy analysis are trending and inspiring many scientists; likewise, we also studied disease models with risk analysis using fuzzy logic, which is the motivation for our work also [40]. Literature on disease modeling with fuzzy system is also little less in number, so we proposed the fuzzy SVIRS disease system with Holling type-II functional response. The current model is studied under fuzzy system and studied analytically and numerically using mathematical and computer software tools, respectively [41]. This work focused on parameter analysis also to analyze all parameters numerically to identify, which parameter influences and effects the system strongly [42]. The current work focused on the fuzzy system for the SVIRS disease model with Holling type-II functional response. All disease models are driven from the basic disease model SIR and SIER [43]. These models are very basic in nature. To capture disease detection, disease transmission, and risk analysis, we need to study the model with little complex constraints which may be interactions (like functional responses) which are complex in nature [44]. To serve an optimal solution for disease detection, disease transmission and its stages and recovery status and its stages can be achieved greatly by fuzzy systems. The fuzzy system works greatly when the scenario is complex in nature, uncertainty in scenario, and vague data are involved.

The parameters used to mathematically express biological events are typically assumed to be accurate. Researchers have only made a few attempts to include environmental uncertainty into their research. The application of diverse mathematical approaches and concepts aids in the better understanding of biological and physical processes. In biological modeling, interval parameters or fuzzy parameters should be employed more frequently than recent attempts due to the realistic scenario. The fuzzy set theory, proposed by Zadeh [40], can be used to account for uncertainty in biological data. The application of fuzzy logic and fuzzy sets in biological systems offers a lot of potential, but there are not many of them. Reference [45] has several examples of fuzzy mathematics applications. Angalaeswari et al. describe some epidemic models that take into account parameter uncertainty and population heterogeneity [45]. We investigated a fuzzy SVIRS diseases system with Holling type-II incidence rate and saturated therapy based on the motivation of [30–36, 46], in which all parameters linked to population dynamics were considered as fuzzy numbers. The current work is definitely different previous works in view of parameter analysis, which says the control parameters for disease transmission and recovery greatly. Fuzzy analysis definitely added strength to the current work which shapes it as a novel innovative and informative study. Certainly, this work can contribute qualitative information and notable conclusions to the literature.

2. Preliminaries of Fuzzy Analysis

A fuzzy set is a collection of things in which there is no clear distinction between those that belong to the group and those that do not. We will go over some basic notations for fuzzy sets in this section [46]. We recommend Natrayan [47] and Klir and Yuan [48] for further information on fuzzy sets.

Definition 1. ζ-cut of a fuzzy number: a nonempty set P, a fuzzy set in P is a map $f: P \longrightarrow [0, 1]$. A ζ-cut of a fuzzy number $\widetilde{f}$ in P is denoted by $f_\zeta = [f_l(\zeta), f_u(\zeta)]$, where

$f_1(\zeta)$and $f_u(\zeta)$ are the lower and upper bounds of the closed interval in that order and is defined as the following fuzzy set [49]:

$$f_\zeta = \left\{ \frac{p}{\Xi_{\widetilde{f}}(p) \geq \zeta, p \in P} \right\} \text{where } \zeta \in [0,1]. \tag{1}$$

Figure 1 shows the ζ-cut of a triangular fuzzy number. Figure 2 shows the triangular fuzzy number.

Definition 2. Triangular fuzzy number.

A triangular fuzzy number is a continuous membership function $\Xi_{\widetilde{f}}(p)$: $P \longrightarrow [0,1]$ and is denoted by $\widetilde{f}$.

Definition 3. Utility function method.

The utility function is defined as the weighted sum of the objectives:

$$U = \sum_{k=1}^{n} \sigma_i f_i, \sigma_i \geq 0, \tag{2}$$

where σ_i is a scalar that represents the relative importance of the objectives f_i and subject to the condition $\sum_{k=1}^{n} f_i = 1$.

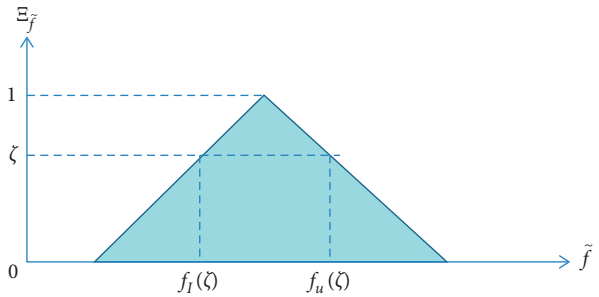

Figure 1: ζ-cut of a triangular fuzzy number.

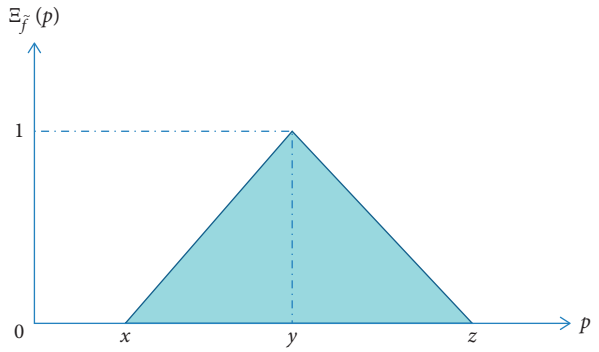

Figure 2: Triangular fuzzy number.

3. Fuzzy Model

Let $\widetilde{S}(t), \widetilde{V}(t), \widetilde{I}(t)$, and $\widetilde{R}(t)$ denote the population densities of fuzzy susceptible, vaccinated, infected, and recovered human in the environment at time t, respectively. By using the concept on the fuzzy initial value problem [1] and differentials of fuzzy functions [2] and considering a set of fuzzy differential equations regarding the following SVIRS model [50], Table 1 shows the physical description of the symbols. Figure 3 shows the schematic diagram of the SVIRS fuzzy model.

$$\begin{cases} D\widetilde{S} = \widetilde{\Delta} - \widetilde{\Omega}S - \dfrac{\widetilde{\alpha}SI}{1+\widetilde{\beta}I} - \widetilde{\gamma}S = \widetilde{\phi}R, \\ D\widetilde{V} = \widetilde{\Omega}S - \dfrac{\widetilde{\chi}SI}{1+\widetilde{\beta}I} - \widetilde{\gamma}V, \\ D\widetilde{I} = \dfrac{\widetilde{\alpha}SI}{1+\widetilde{\beta}I} + \dfrac{\widetilde{\chi}SI}{1+\widetilde{\beta}I} - (\widetilde{\gamma}+\widetilde{\eta}+\widetilde{\psi})I - \dfrac{\widetilde{m}I}{1+\widetilde{n}I}, \\ D\widetilde{R} = \widetilde{\psi}I + \dfrac{\widetilde{m}I}{1+\widetilde{n}I} - \widetilde{\phi}R - \widetilde{\gamma}R, \end{cases} \tag{3}$$

where $D \equiv \mathrm{d}/\mathrm{d}t$.

Let the solution of the fuzzy system (1) can be defined as $[D\widetilde{Z}]_\sigma = [(DZ)_l^\sigma, (DZ)_u^\sigma]$, then the deterministic system of the fuzzy model (1) is given by

$$\begin{cases} [DS]_l^\sigma = [\Delta_l]^\sigma - [(\delta_u)^\sigma + (\gamma_u)^\sigma]S - \dfrac{(\alpha_u)^\sigma SI}{1+(\beta_l)^\sigma I} + [\phi_l]^\sigma, \\ [DS]_u^\sigma = [\Delta_u]^\sigma - [(\delta_l)^\sigma + (\gamma_l)^\sigma]S - \dfrac{(\alpha_l)^\sigma SI}{1+(\beta_u)^\sigma I} + [\phi_u]^\sigma, \\ [DV]_l^\sigma = [\delta_l]^\sigma S - \dfrac{(\chi_u)^\sigma VI}{1+(\beta_l)^\sigma I} - (\gamma_u)^\sigma V, \\ [DV]_u^\sigma = [\delta_u]^\sigma S - \dfrac{(\chi_l)^\sigma VI}{1+(\beta_u)^\sigma I} - (\gamma_l)^\sigma V, \\ [DI]_l^\sigma = \dfrac{(\alpha_l)^\sigma SI}{1+(\beta_u)^\sigma I} + \dfrac{(\chi_l)^\sigma VI}{1+(\beta_u)^\sigma I} \\ \qquad -[(\gamma_u)^\sigma + (\eta_u)^\sigma + (\psi_u)^\sigma]I - \dfrac{(m_u)^\sigma I}{1+(b_l)^\sigma I}, \\ [DI]_l^\sigma = \dfrac{(\alpha_u)^\sigma SI}{1+(\beta_l)^\sigma I} + \dfrac{(\chi_u)^\sigma VI}{1+(\beta_l)^\sigma I} \\ \qquad -[(\gamma_l)^\sigma + (\eta_l)^\sigma + (\psi_l)^\sigma]I - \dfrac{(m_l)^\sigma I}{1+(b_u)^\sigma I}, \\ [DR]_l^\sigma = (\psi_l)^\sigma I + \dfrac{(m_l)^\sigma I}{1+(n_u)^\sigma I} - [(\phi_u)^\sigma + (\gamma_u)^\sigma]R, \\ [DR]_u^\sigma = (\psi_u)^\sigma I + \dfrac{(m_u)^\sigma I}{1+(n_l)^\sigma I} - [(\phi_l)^\sigma + (\gamma_l)^\sigma]R. \end{cases} \tag{4}$$

Table 1: Physical description of the symbols.

Fuzzy parameters	Description of the symbols
$\tilde{\Delta}$	The recruitment rate of susceptible
$\tilde{\alpha}$	The vigor of infection
$\tilde{\beta}$	The reticence actions taken by the infected
$\tilde{\chi}$	The rate at which vaccinated persons become infected
$\tilde{\Omega}$	The transmission rate from susceptible individuals to vaccinated ones
$\tilde{\phi}$	The transmission rate from recovered individuals to susceptible ones
$\tilde{\Psi}$	The transmission rate from infected individuals to recovered ones
$\tilde{\gamma}$	The natural fatality rate of all the individuals
$\tilde{\eta}$	The death rate due to disease
$\tilde{m}$	The treatment rate
$\tilde{n}$	The rate of limitation in medical resource

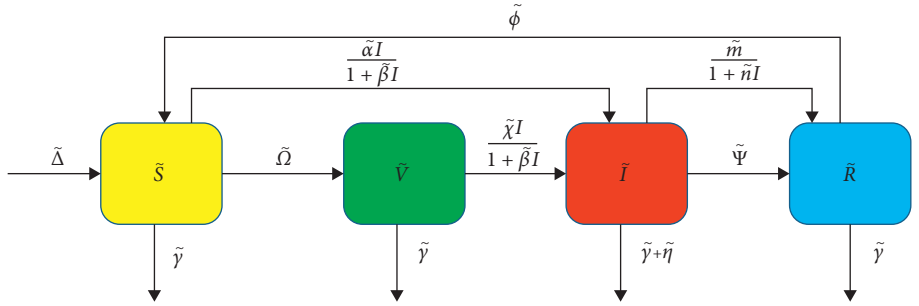

Figure 3: A schematic diagram of the SVIRS fuzzy model.

The above system of differential equations can be solved using the UFM principle as follows [51]:

$$\begin{cases} DS = \sigma_1 [DS]_l^{\sigma} + \sigma_2 [DS]_u^{\sigma}, \\ DV = \sigma_1 [DS]_l^{\sigma} + \sigma_2 [DS]_u^{\sigma}, \\ DI = \sigma_1 [DS]_l^{\sigma} + \sigma_2 [DS]_u^{\sigma}, \\ DR = \sigma_1 [DS]_l^{\sigma} + \sigma_2 [DS]_u^{\sigma}, \end{cases} \tag{5}$$

where σ_1 and σ_2 are two weight functions such that $\sigma_1 + \sigma_2 = 1$ and $\sigma_1 + \sigma_2 \geq 0$; then, (5) can be written as

$$\begin{cases} DS = u_{11} - u_{12}SI - u_{13}S + u_{14}R, \\ DV = u_{21}S - u_{22}VI - u_{23}V, \\ DI = u_{31}SI - u_{32}VI - u_{13}I + u_{34}I, \\ DR = u_{41}I - u_{42}I - u_{43}R, \end{cases} \tag{6}$$

where

$$\begin{aligned} &u_{11} = \sigma_1 (\Delta_l)^{\sigma} + \sigma_2 (\Delta_u)^{\sigma}; u_{12} = \sigma_1 \frac{(\alpha_u)^{\sigma}}{1 + (\beta_l)^{\sigma} I} + \sigma_2 \frac{(\alpha_l)}{1 + (\beta_u)^{\sigma} I}; u_{14} = \sigma_1 (\phi_l)^{\sigma} + \sigma_2 (\phi_u)^{\sigma}, \\ &u_{13} = \sigma_1 [(\delta_u)^{\sigma} + (\gamma_u)^{\sigma}] + \sigma_2 [(\delta_l)^{\sigma} + (\gamma_u)^{\sigma}]; u_{21} = \sigma_1 (\delta_l)^{\sigma} + \sigma_2 (\delta_u)^{\sigma}, \\ &u_{22} = \sigma_1 \frac{(\chi_u)^{\sigma}}{1 + (\beta_u)} + \sigma_2 \frac{(\chi_l)^{\sigma}}{1 + (\beta_l)}; u_{23} = \sigma_2 (\gamma_u)^{\sigma} + \sigma_2 (\gamma_l)^{\sigma}; u_{31} = \sigma_1 \frac{(\alpha_l)^{\sigma}}{1 + (\beta_u)} + \sigma_2 \frac{(\alpha_u)^{\sigma}}{1 + (\beta_l)}, \\ &u_{32} = \sigma_1 \frac{(\chi_u)^{\sigma}}{1 + (\beta_u)} + \sigma_2 \frac{(\chi_l)^{\sigma}}{1 + (\beta_l)}; u_{34} = \sigma_1 \frac{(m_u)^{\sigma}}{1 + (n_l)^{\sigma} I} + \sigma_2 \frac{(m_l)^{\sigma}}{1 + (n_u)^{\sigma} I}, \\ &u_{33} = \sigma_1 [(\gamma_u)^{\sigma} + (\eta_u)^{\sigma} + (\psi_u)^{\sigma}] + \sigma_2 [(\gamma_l)^{\sigma} + (\eta_l)^{\sigma} + (\psi_l)^{\sigma}]; u_{41} = \sigma_1 (\psi_l)^{\sigma} + \sigma_2 (\psi_u)^{\sigma}, \\ &u_{22} = \sigma_1 \frac{(m_l)^{\sigma}}{1 + (n_u)^{\sigma}} + \sigma_2 \frac{(m_u)^{\sigma}}{1 + (n_l)^{\sigma}}; u_{43} = \sigma_1 (\phi_u)^{\sigma} + \sigma_2 (\phi_l)^{\sigma}; u_{44} = \sigma_1 (\gamma_u)^{\sigma} + \sigma_2 (\gamma_l)^{\sigma}. \end{aligned} \tag{7}$$

4. Positivity and Boundedness of the SVIRS Fuzzy Model

In this section, all solutions of the proposed system (3) have been bounded [52]. First, we use Lemma 1 to verify the positivity of system (3).

Lemma 1. *If* $u_{13}-u_{21}>0, u_{43}-u_{14}>0, u_{34}-u_{33}-u_{41}-u_{42}>0, u_{31}-u_{12}>0, u_{32}-u_{22}>0$ *provided that* $(\delta_l)^\sigma+(\gamma_l)^\sigma>(\delta_u)^\sigma$, $(\phi_l)^\sigma>(\phi_u)^\sigma$, $(m_l)^\sigma/1+(n_u)^\sigma+(\gamma_l)^\sigma+(\eta_l)^\sigma+(\varphi_l)^\sigma>(\varphi_u)^\sigma+(m_u)^\sigma/1+(n_l)^\sigma$, $(\alpha_u)^\sigma/1+(\beta_l)^\sigma>(\delta_u)^\sigma$, *then the solutions* $S(t)$, $V(t)$,$I(t)$, *and* $R(t)$ *of system (3) are positives.*

Proof. Consider

$$\begin{cases} u_{13}-u_{21}=\sigma_1\left[(\delta_u)^\sigma+(\gamma_u)^\sigma\right]+\sigma_2\left[(\delta_l)^\sigma+(\gamma_l)^\sigma\right] \\ -\sigma_1(\delta_l)^\sigma-\sigma_2(\delta_u)^\sigma \\ =\sigma_1\{2(\delta_u)^\sigma+(\gamma_u)^\sigma-2(\delta_l)^\sigma+(\gamma_l)^\sigma\} \\ +(\delta_l)^\sigma+(\gamma_l)^\sigma-\sigma_2(\delta_u)^\sigma. \end{cases} \tag{8}$$

Now, $\sigma_1=0$, we have $u_{31}-u_{21}=(\delta_l)^\sigma+(\gamma_l)^\sigma-(\delta_u)^\sigma$; then, $u_{13}-u_{21}$ will be positive for $\sigma_1=0$ if

$$(\delta_l)^\sigma+(\gamma_l)^\sigma>(\delta_u)^\sigma. \tag{9}$$

Therefore, from equation (8), it is obtained that

$$\frac{d}{d\sigma_1}(u_{13}-u_{21})=\{2(\delta_u)^\sigma+(\gamma_u)^\sigma-2(\delta_l)^\sigma+(\gamma_l)^\sigma\}>0, \quad \forall\sigma_1\in[0,1]. \tag{10}$$

So, $u_{13}-u_{21}$ is an increasing function with respect to σ_1, and it will be positive if condition (9) holds. In the similar way, it can be proved that $u_{43}-u_{14}, u_{33}+u_{34}-u_{41}-u_{42}$ is an increasing function with respect to σ_1, and it will be positive if the condition $(\phi_l)^\sigma>(\phi_u)^\sigma+(\psi_1)^\sigma>(m_l)^\sigma/1+(n_u)^\sigma+(\gamma_l)^\sigma+(\eta_l)^\sigma+(\psi_l)^\sigma>(\psi_u)^\sigma+(m_u)^\sigma/1+(n_l)^\sigma$, $(\alpha_u)^\sigma/1+(\beta_l)^\sigma>(\delta_u)^\sigma$, $(\chi_u)^\sigma/1+(\beta_l)^\sigma>(\chi_l)^\sigma/1+(\beta_u)^\sigma$ holds. □

Theorem 1. *All solutions of system (3) are bounded in the region* R_+^4 *provided that*

$$u_{31}>u_{12}, u_{32}>u_{22}, \quad \mu=\min\{u_{23}, u_{13}-u_{21}, u_{43}-u_{14}, u_{33}+u_{34}-u_{41}-u_{42}\}. \tag{11}$$

Proof. Let us define a function $G=S+V+I+R$.

Now, by separating and simplifying with regard to time t, we have

$$DG=DS+DV+DI+DR,$$

$$\begin{cases} DG=u_{11}-u_{23}V+(u_{21}-u_{13})S \\ +(u_{41}+u_{42}-u_{34}-u_{33})I \\ +(u_{14}-u_{43})R+(u_{31}-u_{12})SI \\ +(u_{32}-u_{22})VI. \end{cases} \tag{12}$$

For a positive real number μ,

$$\begin{aligned} DG+\mu G=&\ u_{11}+[\mu-u_{23}]V+[\mu-(u_{13}-u_{21})]S \\ &+[\mu-(u_{34}+u_{33}-u_{41}-u_{42})]I \\ &+[\mu-(u_{43}-u_{14})]R \\ &+(u_{31}-u_{21})SI+(u_{32}-u_{22})VI. \end{aligned} \tag{13}$$

Now, according to Lemma 1, if $\mu=\min\{u_{23}, u_{13}-u_{21}, u_{43}-u_{14}, u_{34}+u_{33}-u_{41}-u_{42}\}$, then the above equation becomes $DG+\mu G\le u_{11}$. Solving this, we get $G\le u_{11}/\mu+ke^{-\mu t}$. As $t\longrightarrow\infty$, we have $G\le u_{11}/\mu$. So, it can show $S(t)\le u_{11}/\mu, V(t)\le u_{11}/\mu, I(t)\le u_{11}/\mu, R(t)\le u_{11}/\mu$. This establishes that the system's solution is bounded.

The solutions of system (3) are bounded in the region R_+^4 provided that $a_{31}>a_{12}$, $a_{32}>a_{22}$ and $\mu=\min\{u_{23}, u_{13}-u_{21}, u_{43}-u_{14}, u_{33}+u_{34}-u_{41}-u_{42}\}\sigma_1=0$. □

5. Existence and Stability Analysis

In this section, we look at the presence and stability of the fuzzy system's nonnegative equilibrium point (3). In a fuzzy system (3), there are two nonnegative equilibrium points. The following are the existence and stability conditions for them [53]:

(i) Disease free equilibrium point $P_1(S^0,0,0,0)=(u_{11}/u_{13},0,0,0)$

(ii) Endemic equilibrium point $P_2(S^*,V^*,I^*,R^*)$

Here, $S^*=u_{11}u_{43}+u_{14}u_{11}+u_{14}u_{42}/u_{43}u_{13}+u_{43}u_{12}I^*$, $V^*=u_{21}u_{11}u_{43}+u_{21}u_{14}u_{41}+u_{21}u_{14}u_{42}/u_{43}u_{12}u_{22}I^*+u_{43}u_{13}u_{22}I^*+u_{43}u_{12}u_{23}I^*+u_{43}u_{13}u_{23}$,

$$R^*=\frac{u_{41}+u_{42}}{u_{43}}I^*, \qquad \Gamma_1I^{*2}+\Gamma_2I^*+\Gamma_3=0, \tag{14}$$

where

$$\begin{aligned} \Gamma_1=&\ u_{12}u_{22}u_{33}u_{43}+u_{12}u_{22}u_{34}u_{43}, \\ \Gamma_2=&\ u_{13}u_{22}u_{33}u_{43}+u_{13}u_{22}u_{34}u_{43}+u_{12}u_{23}u_{33}u_{43} \\ &+u_{12}u_{23}u_{34}u_{43}-u_{11}u_{22}u_{31}u_{43} \\ &-u_{22}u_{31}u_{14}u_{41}-u_{14}u_{22}u_{31}u_{42}, \\ \Gamma_3=&\ u_{13}u_{23}u_{33}u_{43}+u_{13}u_{23}u_{34}u_{43}-u_{11}u_{31}u_{23}u_{43} \\ &-u_{14}u_{31}u_{23}u_{41}-u_{14}u_{31}u_{23}u_{42}-u_{11}u_{21}u_{32}u_{43} \\ &-u_{14}u_{21}u_{32}u_{41}-u_{14}u_{21}u_{32}u_{42}. \end{aligned} \tag{15}$$

Theorem 2. *Fuzzy system (3) is locally asymptotically stable at disease free equilibrium point* $P_1(S^0,0,0,0)$ *if* $u_{13}^2-u_{11}u_{13}>0$ *and* $u_{13}u_{44}-u_{11}u_{31}>0$*; otherwise, it is unstable.*

Proof. The characteristic equation of the fuzzy system (3) at disease free equilibrium point $P_1(S^0,0,0,0)$ is

$$\lambda^4 + \sum_1 \lambda^3 + \sum_2 \lambda^2 + \sum_3 \lambda + \sum 4 = 0, \tag{16}$$

where

$$\begin{aligned}
\sum 1 &= u_{13} + u_{23} + u_{33} + u_{43} + u_{44} - u_{31}S^0,\\
\sum 2 &= u_{13}u_{43} + u_{13}u_{33} + u_{13}u_{44} + u_{23}u_{43} + u_{23}u_{33}\\
&\quad + u_{23}u_{44} + u_{13}u_{23} - u_{31}u_{13}S^0 - u_{23}u_{31}S^0,\\
\sum 3 &= u_{13}u_{33}u_{43} + u_{13}u_{43}u_{44} + u_{23}u_{33}u_{43} + u_{23}u_{43}u_{44}\\
&\quad + u_{23}u_{43}u_{13} + u_{23}u_{33}u_{13} + u_{23}u_{13}u_{44}\\
&\quad - u_{23}u_{31}u_{43}S^0 - u_{23}u_{31}u_{13}S^0,\\
\sum 4 &= u_{13}u_{33} + u_{13}u_{44} - u_{31}u_{13}S^0.
\end{aligned} \tag{17}$$

The required and sufficient requirements for local stability of a disease-free equilibrium point $p_1(S^0, 0, 0, 0)$ according to Routh–Hurwitz criteria if $\sum 1 > 0$, $\sum 3 > 0$, $\sum 4 > 0$, $\sum 3(\sum 1 \sum 2 - \sum 3) > \sum_1^2 \sum 4$, and $\sum_4 (\sum_1 \sum_2 \sum_3 - \sum_1^2 \sum_4 - \sum_3^2) > 0$. It is evident that $u_{13}^2 - u_{11}u_{13} > 0$ and $u_{13}u_{44} - u_{11}u_{31} > 0$. □

Theorem 3. *Fuzzy system (3) is locally asymptotically stable at endemic equilibrium point $p_2(S^*, V^*, I^*, R^*)$ if $S^* < max\{u_{13}/u_{31}, u_{33}/u_{31}\}$, $V^* < max\{u_{23}/u_{32}, u_{34}/u_{32}\}$, $u_{33} - u_{31} > 0$, $u_{22} - u_{12} > 0, u_{12}u_{23}u_{33} > u_{14}u_{31}(u_{41} + u_{42})$, $u_{12}u_{23}u_{33}u_{43} > u_{14}u_{22}u_{31}(u_{41} + u_{42})$; otherwise, it is unstable [54].*

Proof. The characteristic equation of fuzzy system (3) at the endemic equilibrium point $p_2(S^*, V^*, I^*, R^*)$ is

$$\lambda^4 + \Theta_1\lambda^3 + \Theta_2\lambda^2 + \Theta_3\lambda + \Theta_4 = 0, \tag{18}$$

where

$$\begin{aligned}
\Theta_1 &= u_{13} + u_{23} + u_{33} + u_{34} + u_{43} + u_{12}I^* + u_{22}I^* - u_{31}S^* - u_{32}V^*,\\
\Theta_2 &= u_{13}u_{23} + u_{13}u_{33} + u_{13}u_{34} + u_{23}u_{43} + u_{23}u_{34}\\
&\quad + u_{23}u_{43} + u_{33}u_{43} + u_{34}u_{43} + u_{12}u_{23}I^* + u_{12}u_{33}I^*\\
&\quad + u_{12}u_{34}I^* + u_{12}u_{43}I^* + u_{13}u_{22}I^* + u_{22}u_{33}I^*\\
&\quad + u_{22}u_{34}I^* + u_{22}u_{43}I^* - u_{13}u_{31}S^* - u_{23}u_{31}S^*\\
&\quad - u_{31}u_{43}S^* - u_{13}u_{32}V^* - u_{23}u_{32}V^*\\
&\quad - u_{32}u_{43}V^*I^* - u_{22}u_{31}S^*I^*,\\
\Theta_3 &= u_{13}u_{23}u_{33} + u_{13}u_{23}u_{34} + u_{13}u_{23}u_{43} + u_{13}u_{33}u_{43} + u_{13}u_{43}u_{34}\\
&\quad + u_{33}u_{23}u_{43} + u_{43}u_{23}u_{34} - u_{31}u_{14}u_{42}I^* - u_{14}u_{31}u_{41}I^*\\
&\quad + u_{22}u_{34}u_{43}I^* + u_{22}u_{33}u_{43}I^* + u_{13}u_{22}u_{43}I^* + u_{13}u_{22}u_{34}I^*\\
&\quad + u_{13}u_{33}u_{22}I^* + +u_{22}u_{34}u_{43}I^* + u_{22}u_{33}u_{43}I^* + u_{13}u_{22}u_{43}I^*\\
&\quad + u_{13}u_{22}u_{34}I^* + u_{13}u_{33}u_{22}I^* + u_{13}u_{33}u_{22}I^* + u_{12}u_{34}u_{43}I^*\\
&\quad + u_{12}u_{33}u_{43}I^* + u_{12}u_{23}u_{33}I^* - u_{31}u_{23}u_{43}S^* - u_{23}u_{43}u_{32}V^*\\
&\quad + u_{22}u_{34}u_{43}I^* - u_{13}u_{23}u_{31}S^* - u_{13}u_{23}u_{32}V^* - u_{13}u_{31}u_{43}S^*\\
&\quad - u_{13}u_{43}u_{32}V^* + u_{12}u_{22}u_{34}I^{*2} + u_{12}u_{22}u_{43}I^{*2} - u_{12}u_{23}u_{32}V^*I^*\\
&\quad - u_{12}u_{31}u_{43}S^*I^* - u_{31}u_{22}u_{43}S^*I^* + u_{12}u_{23}u_{32}VI^{*2} + u_{21}u_{12}u_{32}S^*I^*\\
&\quad + u_{12}u_{22}u_{33}S^*I^{*2} + u_{12}u_{31}u_{43}S^*I^* - u_{12}u_{22}u_{31}S^*I^{*2},\\
\Theta_4 &= u_{13}u_{23}u_{33}u_{43} + u_{13}u_{23}u_{33}u_{43} + u_{13}u_{23}u_{34}u_{43} + u_{12}u_{23}u_{34}u_{43}I^*\\
&\quad - u_{14}u_{23}u_{31}u_{41}I^* - u_{14}u_{23}u_{31}u_{42}I^* + u_{13}u_{22}u_{33}u_{43}I^* + u_{13}u_{22}u_{34}u_{43}I^*\\
&\quad - u_{14}u_{21}u_{32}u_{41}I^* - u_{14}u_{23}u_{32}u_{42}I^* - u_{13}u_{23}u_{31}u_{43}S^* - u_{13}u_{23}u_{32}u_{43}V^*\\
&\quad + u_{13}u_{23}u_{33}u_{43}I^* - u_{13}u_{23}u_{31}u_{43}S^* - u_{13}u_{23}u_{32}u_{43}V^* + u_{12}u_{22}u_{32}u_{43}V^*I^{*^2}\\
&\quad - u_{13}u_{22}u_{31}u_{43}S^*I^* - u_{12}u_{23}u_{32}u_{43}V^*I^* + u_{12}u_{22}u_{33}u_{43}I^{*^2} + u_{12}u_{32}u_{22}u_{43}V^*I^{*^2}\\
&\quad + u_{12}u_{22}u_{34}u_{43}I^{*^2} + u_{12}u_{21}u_{32}u_{43}S^*I^* - u_{14}u_{22}u_{31}u_{41}I^{*^2} - u_{14}u_{22}u_{31}u_{42}I^{*^2}.
\end{aligned} \tag{19}$$

The required and sufficient requirements for local stability of a disease-free equilibrium point $p_1(S^0, 0, 0, 0)$ according to the Routh–Hurwitz criteria if $\Theta_1 > 0, \Theta_3 > 0$, $\Theta_4 > 0$, $\Theta_3(\Theta_1\Theta_2 - \Theta_3) > \Theta_1^2\Theta_4$ and $\Theta_4(\Theta_1\Theta_2\Theta_3 - \Theta_1^2\Theta_4 - \Theta_3^2) > 0$.

It is evident that

$$S^* < \mathrm{MAX}\left\{\frac{u_{13}}{u_{31}}, \frac{u_{33}}{u_{31}}\right\}, V^* < \mathrm{MAX}\left\{\frac{u_{23}}{u_{32}}, \frac{u_{34}}{u_{32}}\right\},$$
$$u_{33} - u_{31} > 0, u_{22} - u_{12} > 0,$$
$$u_{12}u_{23}u_{33} > u_{14}u_{31}(u_{41} + u_{42}), \quad (20)$$
$$u_{12}u_{23}u_{33} > u_{14}u_{31}(u_{41} + u_{42}).$$

□

Theorem 4. *Fuzzy system (3) is globally asymptotically stable at the endemic equilibrium point $p_2(S^*, V^*, I^*, R^*)$. If $\aleph_1 > 0$, where*

$$\aleph_1 = u_{31}\aleph + u_{32}\aleph - u_{33} - u_{34} + \min\begin{bmatrix} \{u_{12}\aleph - u_{13} - u_{22}\aleph - u_{23} - \max\{u_{22}\aleph, u_{12}\aleph\}\}, -u_{21} - u_{31}\aleph \\ +\min\{u_{22}\aleph + u_{23}, -u_{32}, \aleph(u_{22} - u_{32}) + u_{33} + u_{34}\} \end{bmatrix}. \quad (21)$$

Proof. Let us consider the subsystem of fuzzy system (3):

$$\begin{cases} DS = u_{11} - u_{12}SI - u_{13}S + u_{14}R, \\ DV = u_{21}S - u_{22}VI - u_{23}V, \\ DI = u_{31}SI + u_{33}VI - u_{33}I - u_{34}I. \end{cases} \quad (22)$$

Let N be the variation matrix of the system (8) is

$$N = \begin{bmatrix} -u_{12}I^* - u_{13} & 0 & -u_{12}S^* \\ u_{21} & -u_{22}I^* - u_{23} & -u_{22}V^* \\ u_{13}I^* & u_{32} & u_{31}S^* + u_{32}V^* - u_{33} - u_{34} \end{bmatrix}. \quad (23)$$

Let $N^{[2]}$ be the second additive compound matrix of N, we have

$$N = \begin{bmatrix} -u_{12}I^* - u_{13} - u_{22}I^* - u_{23} & -u_{22}V^* & -u_{12}S^* \\ u_{32} & -u_{22}I^* - u_{23}u_{31}S^* + u_{32}V^* - u_{33} - u_{34} & 0 \\ u_{13}I^* & u_{21} & -u_{22}I^* - u_{23}u_{31}S^* + u_{32}V^* - u_{33} - u_{34} \end{bmatrix}. \quad (24)$$

Let us consider the function $\prod_x = \partial\prod/\partial x = \mathrm{diag}(\dot{S}/I - S\dot{I}/I^2, \dot{S}/I - S\dot{I}/I^2, \dot{S}/I - S\dot{I}/I^2)$.

Thus, we have $\prod_x \prod^{-1} = \mathrm{diag}(\dot{S}/I - \dot{S}\dot{I}/I, \dot{S}/S - \dot{I}/I^2, \dot{S}/I - \dot{I}/I)$ and $\prod N^{[2]} \prod^{-1} = N^{[2]}$, so that

$$\Xi = \prod_x \prod^1 + \prod N^{[2]} \prod^{-1} = \begin{bmatrix} \Xi_{11} & \Xi_{12} \\ \Xi_{21} & \Xi_{22} \end{bmatrix}, \quad (25)$$

where $\Xi_{11} = \dot{S}/S - \dot{I}/I - u_{12}I^* - u_{13} - u_{22}I^* - u_{23}; \Xi_{12} = [-u_{22}V^* u_{12}S^*]; \Xi_{21} = [u_{21}u_{13}I^*]^T$.

$$\Xi_{22} = \begin{bmatrix} \dot{S}/S - \dot{I}/I - u_{22}I^* - u_{23} - u_{22}V^* \\ u_{32}\dot{S}/S - \dot{I}/I + u_{31}S^* - u_{32}V^* - u_{33} - u_{34} \end{bmatrix}. \quad (26)$$

We considered $\mathfrak{R}$ as the Lozinskii measure by Martin [7] with respect to the norm defined in three-dimensional space $|(x, y, z)| = \max\{|x|, |y + z|\}$, where (x, y, z) is any vector in R^3. Hence, $\mathfrak{R}\{P\} \le \sup\{P_1, P_1\}$, where $P_i = \mathfrak{R}\{\Xi_{ii}\} + |\Xi_{ij}|$ for $i = 1, 2$ and $i \ne j$ and $\mathfrak{R}_1$ denotes the Lozinskii measure with respect to the Γ_1 vector norm. The Lozinskii measure for the matrix Ξ is given by

$$\mathfrak{R}_1(\Xi_{11}) = \frac{\dot{S}}{S} - \frac{\dot{I}}{I} - -u_{12}I^* - u_{13} - u_{22}I^* - u_{23}; |\Xi_{12}|$$
$$= \max\{u_{22}V^*, u_{12}S^*\}$$
$$\Xi_{21} = [u_{21}u_{13}I^*]^T; \mathfrak{R}_1(\Xi_{22}) = \frac{\dot{S}}{S} - \frac{\dot{I}}{I} \quad (27)$$
$$- MIN\{u_{22}I^* + u_{23}, V^*(u_{22} - u_{32}) + u_{33} + u_{34}\}.$$

Here, $P_1 = \mathfrak{R}_1(\Xi_{11}) + |\Xi_{12}| = \dot{S}/S - \dot{I}/I - u_{12}I^* - u_{13} - u_{22}I^* - u_{23} + MAX\{u_{22}V^* + u_{12}S^*\}$ and

$$P_2 = \mathfrak{R}_1(\Xi_{22}) + |\Xi_{21}| = \frac{\dot{S}}{S} - \frac{\dot{I}}{I} - u_{21}I^*$$
$$- \min\{u_{22}I^{\∗} + u_{23}, -u_{32}, V(u_{22} - u_{32}) + u_{33} + u_{34}\}. \quad (28)$$

Thus, we have $\dot{I}/I = u_{31}S + u_{32}V - u_{33} - u_{34}$, so that

$$\mathfrak{R}_1(\Xi) \le \frac{\dot{S}}{S} - u_{31}\aleph - u_{32}\aleph + u_{34} - \min\begin{bmatrix} \{u_{12}\aleph - u_{13} - u_{22}\aleph - u_{23} - \max\{u_{22}\aleph, u_{12}\aleph\}\}, -u_{21} - u_{31}\aleph \\ +\min\{u_{22}\aleph + u_{12}, -u_{32}, \aleph(u_{22} - u_{32}) + u_{33} + u_{34}\} \end{bmatrix}. \quad (29)$$

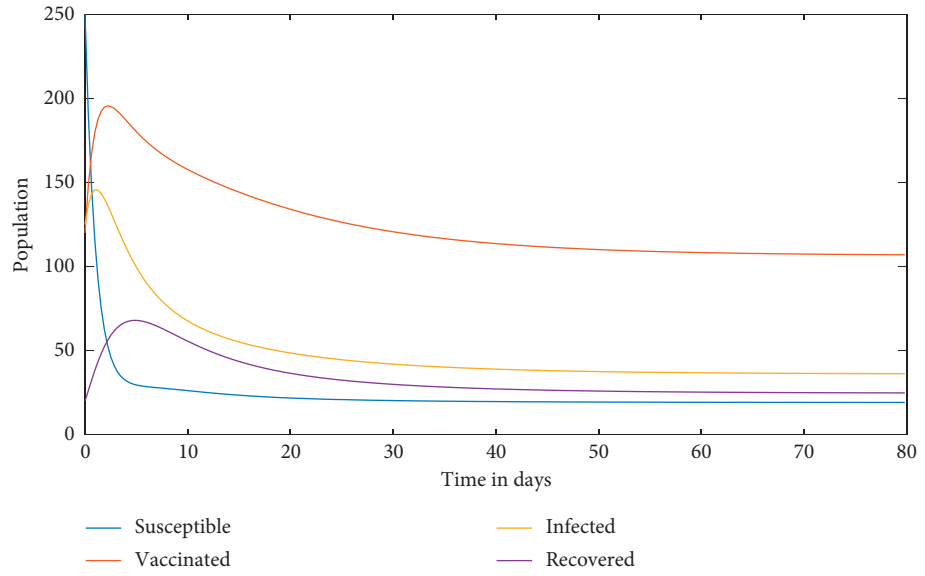

Figure 4: Solution curves of the SVIRS disease system with the attributes in Example 1.

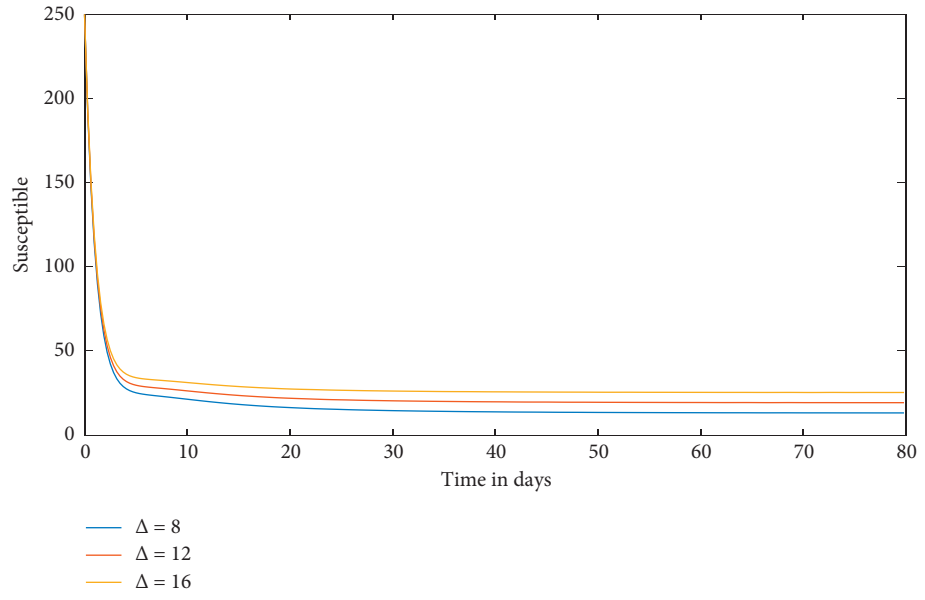

Figure 5: Time series evaluation of susceptible population for the recruitment rates $(\Delta) = 8, 12, 16$.

Since, $\aleph = \min\{\inf S^*(t), \inf V^*(t), \inf I^*(t)\}$, and hence $\Re_1\{\Xi\} \leq S/S - \aleph_1$, where

$$\aleph_1 = u_{31}\aleph + u_{32}\aleph - u_{33} - u_{34} + \min\begin{bmatrix} \{u_{12}\aleph - u_{13} - u_{22}\aleph - u_{23} - \max\{u_{22}\aleph, u_{12}\aleph\}\}, -u_{21} - u_{31}\aleph \\ +\min\{u_{22}\aleph + u_{23}, -u_{23}, \aleph(u_{22} - u_{32}) + u_{33} + u_{34}\} \end{bmatrix}. \tag{30}$$

Now, integrating $\Re_1\{\Xi\}$ w.r.t t' on both sides between the limits 0 to t and on letting $t \longrightarrow \infty$, we obtain $\int_0^t \Re(\Xi)dt = \log S(t)/S(0) - \aleph t \Rightarrow \lim_{t\longrightarrow\infty} \sup\sup 1/t \int_0^t \Re_1(\Xi)dt < -\aleph_1$, if $\aleph_1 > 0$. Therefore, the interior equilibrium point $p_2(S^*, V^*, I^*, R^*)$ will be globally asymptotically stable. □

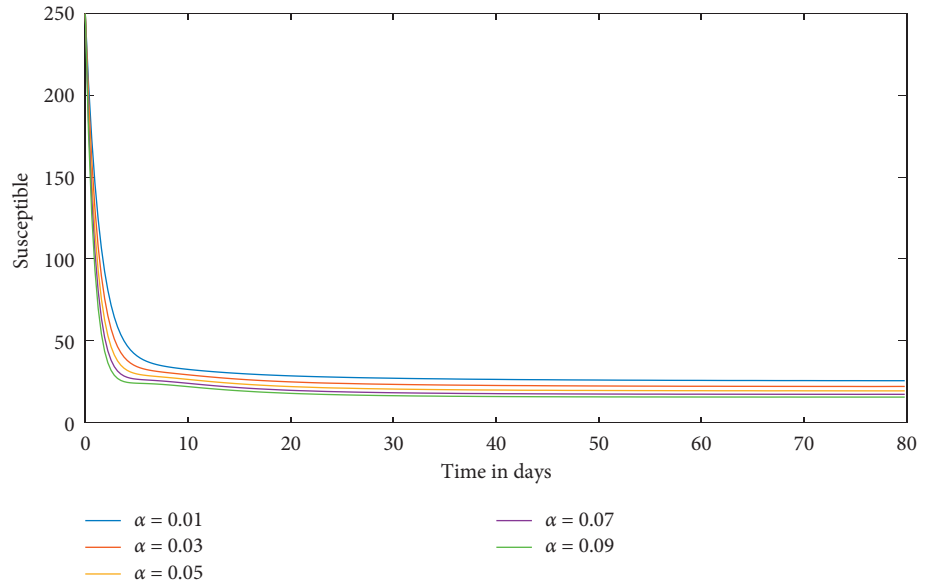

Figure 6: Time series evaluation of susceptible population for $\alpha = 0.01; 0.03; 0.05; 0.07; 0.09$.

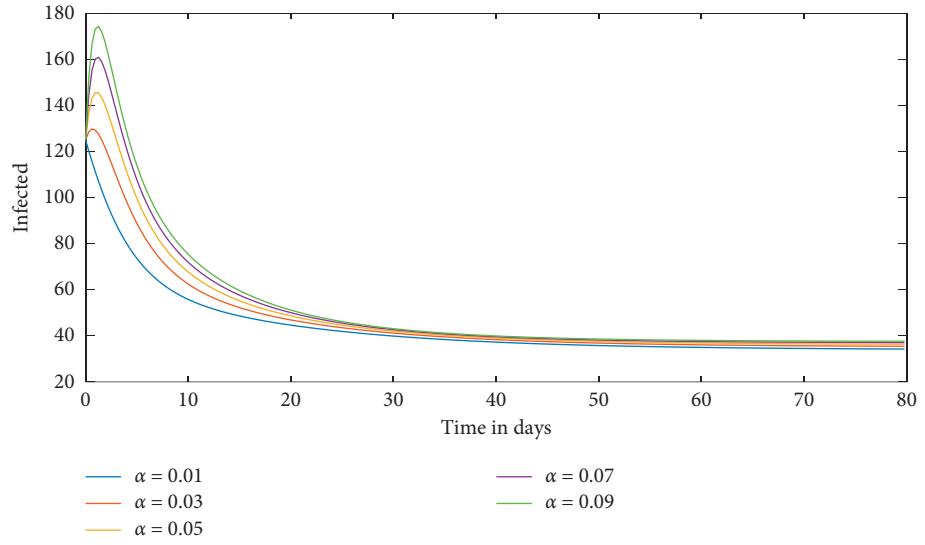

Figure 7: Time series evaluation of infected population for $\alpha = 0.01; 0.03; 0.05; 0.07; 0.09$.

6. Numerical Simulation

In this numerical section, the dynamical behavior of the fuzzy SVIRS system is investigated.

Example 1. The case of endemic equilibrium is illustrated for the following numerical data.

$$\widetilde{\Delta} = [6, 15]; \widetilde{\alpha} = [0.01, 0.09]; \widetilde{\beta} = [0.01, 0.3]; \widetilde{\chi} = [0.005, 0.02]; \widetilde{\Omega} = [0.3, 0.6]; \widetilde{\Phi} = [0.1, 0.5]; \widetilde{\Psi} = [0.1, 0.6]; \widetilde{\gamma} = [0.05, 0.15]; \widetilde{\eta} = [0.01, 0.03]; \widetilde{m} = [1, 8]; \widetilde{n} = [1, 12]. \tag{31}$$

Figure 4 shows solution curves of the SVIRS disease system with the attributes in Example 1. Figure 5 shows time series evaluation of susceptible population for the recruitment rates $(\Delta) = 8, 12, 16$. Figure 6 shows time series evaluation of susceptible population for $\alpha = 0.01; 0.03; 0.05; 0.07; 0.09$. Figure 7 shows time series evaluation of infected population for $\chi = 0.007, 0.009, 0.01, 0.02, 0.03$.

Figure 8 shows time series evaluation of susceptible population for $\beta = 0.05; 0.10; 0.15; 0.20; 0.25$. Figure 9 shows time series evaluation of vaccinated population for

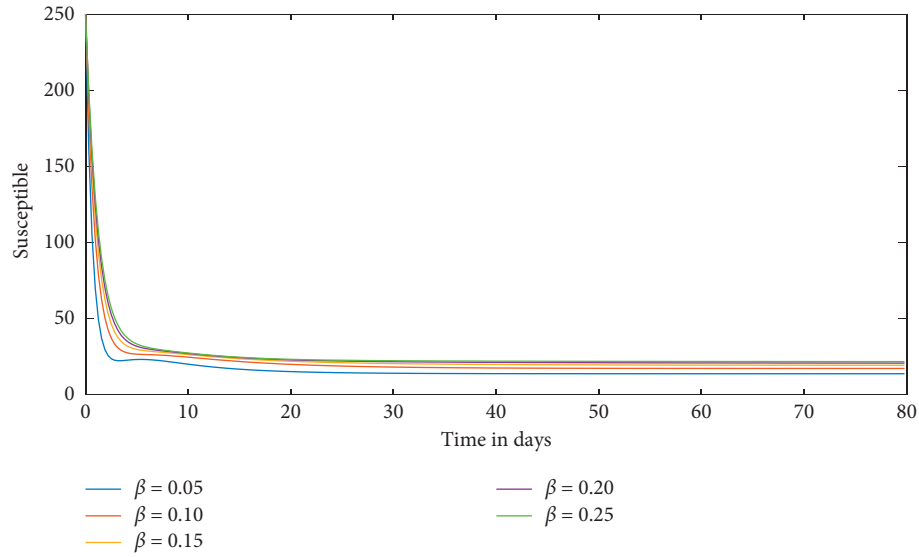

Figure 8: Time series evaluation of susceptible population for $\beta = 0.05; 0.10; 0.15; 0.20; 0.25$.

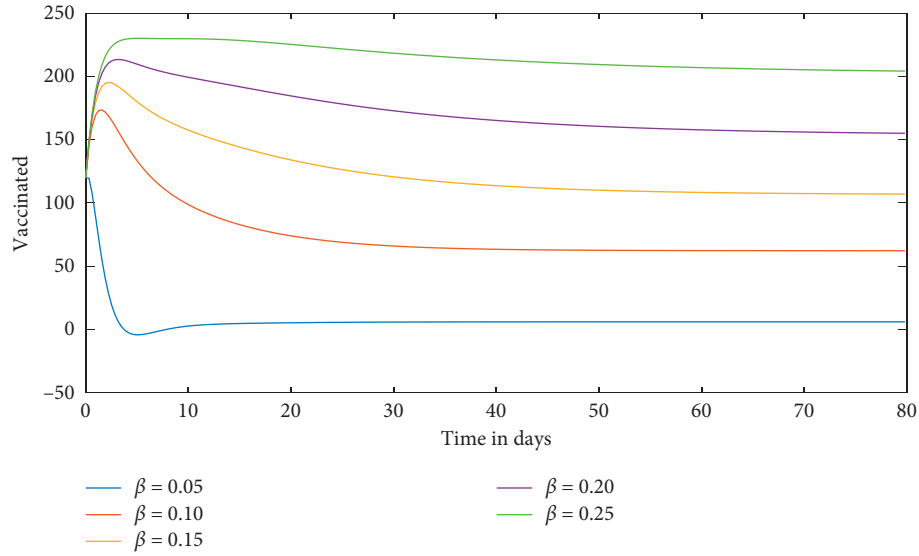

Figure 9: Time series evaluation of vaccinated population for $\beta = 0.05; 0.10; 0.15; 0.20; 0.25$.

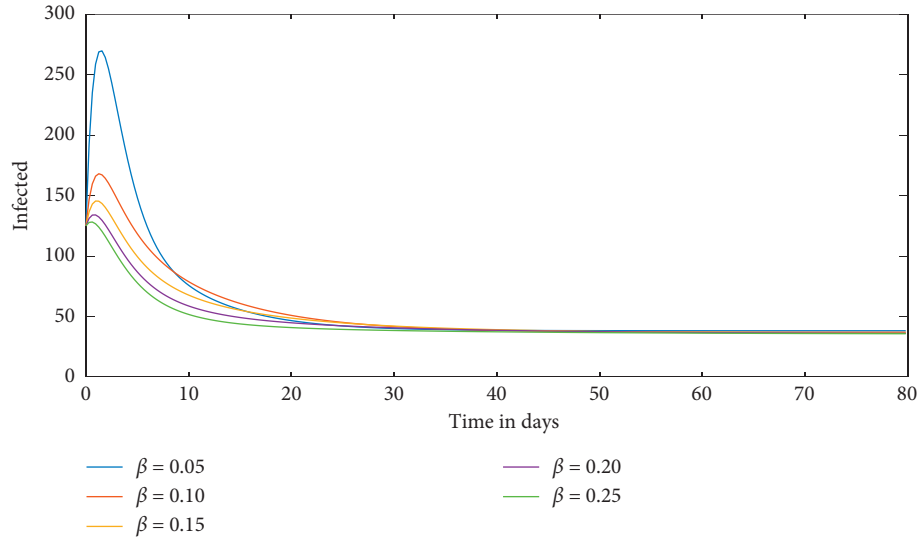

Figure 10: Time series evaluation of infected population for $\beta = 0.05; 0.10; 0.15; 0.20; 0.25$.

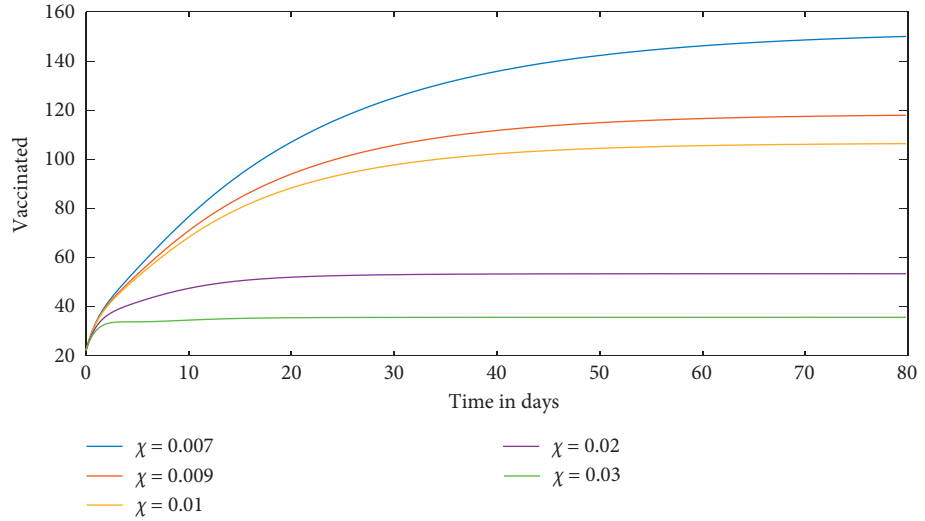

Figure 11: Time series evaluation of vaccinated population for $\chi = 0.007, 0.009, 0.01, 0.02, 0.03$.

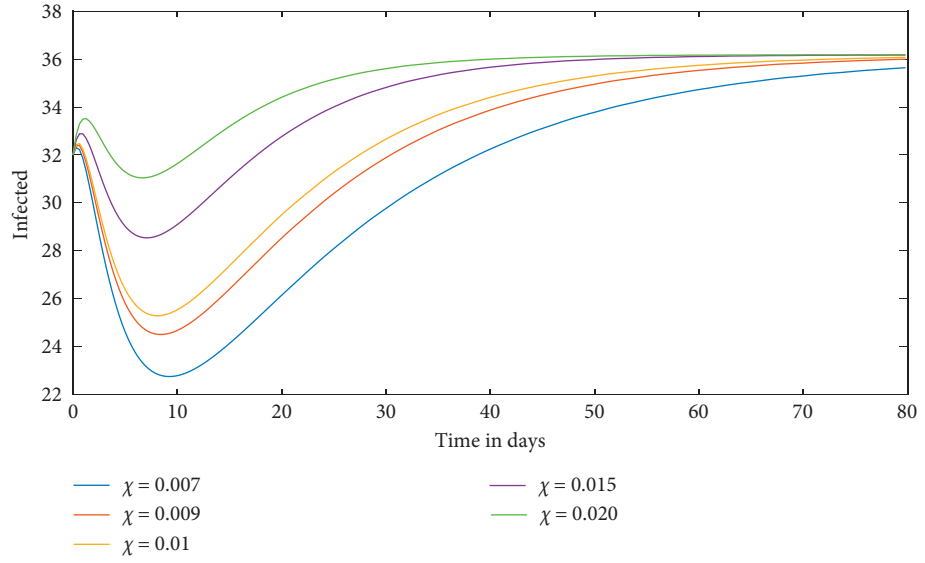

Figure 12: Time series evaluation of infected population for $\chi = 0.007, 0.009, 0.01, 0.02, 0.03$.

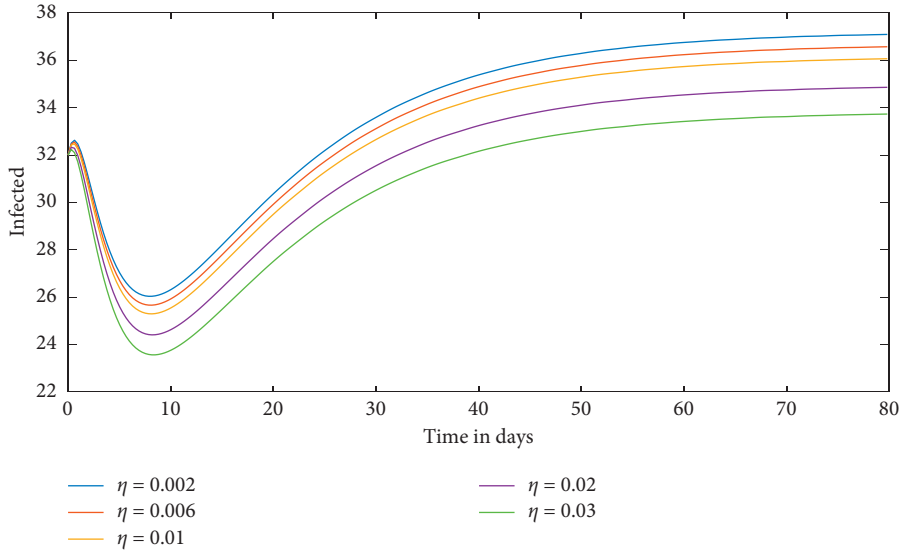

Figure 13: Time series evaluation of infected population for $\eta = 0.002, 0.006, 0.01, 0.02, 0.03$.

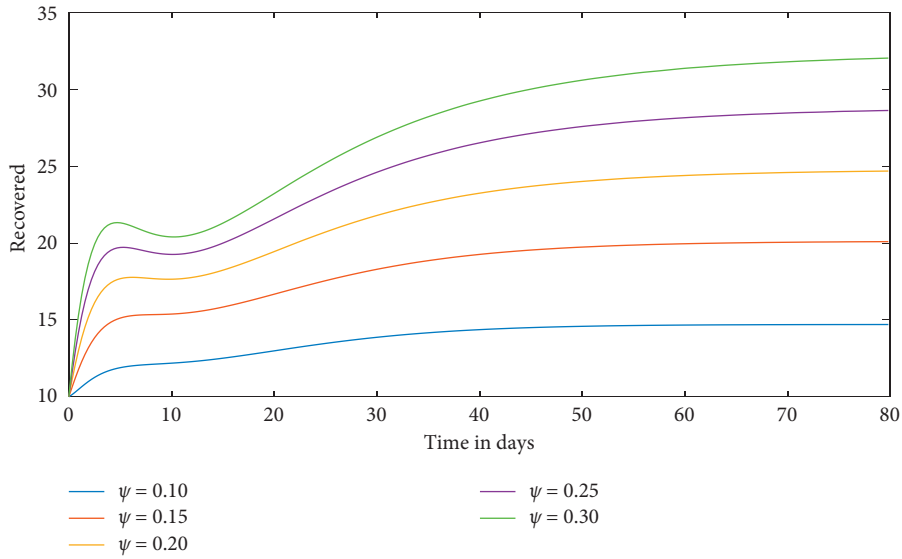

Figure 14: Time series evaluation of recovered population for $\psi = 0.10, 0.15, 0.20, 0.25, 0.30$.

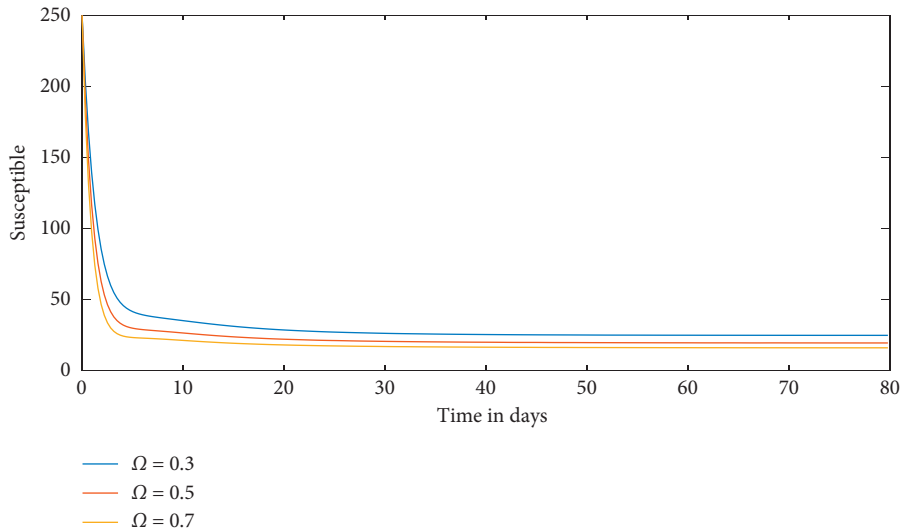

Figure 15: Time series evaluation of susceptible population for $\Omega = 0.3, 0.5, 0.7$.

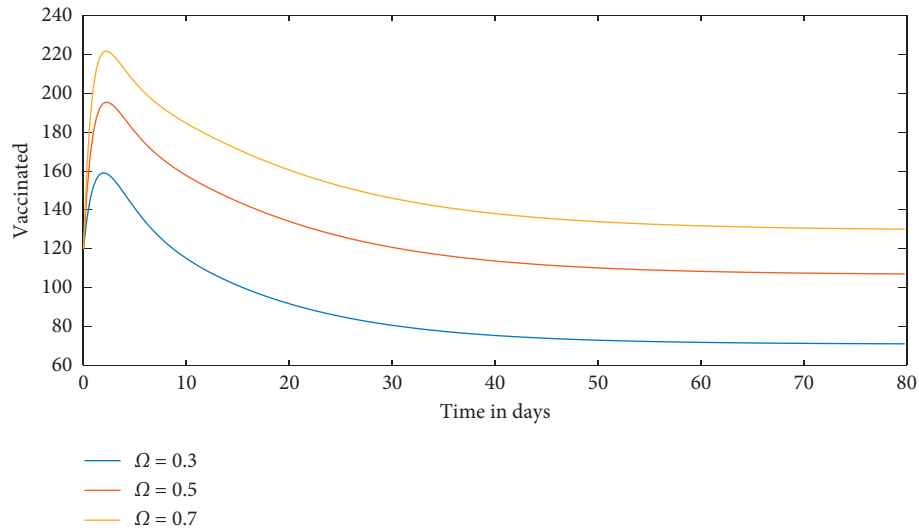

Figure 16: Time series evaluation of vaccinated population for $\Omega = 0.3, 0.5, 0.7$.

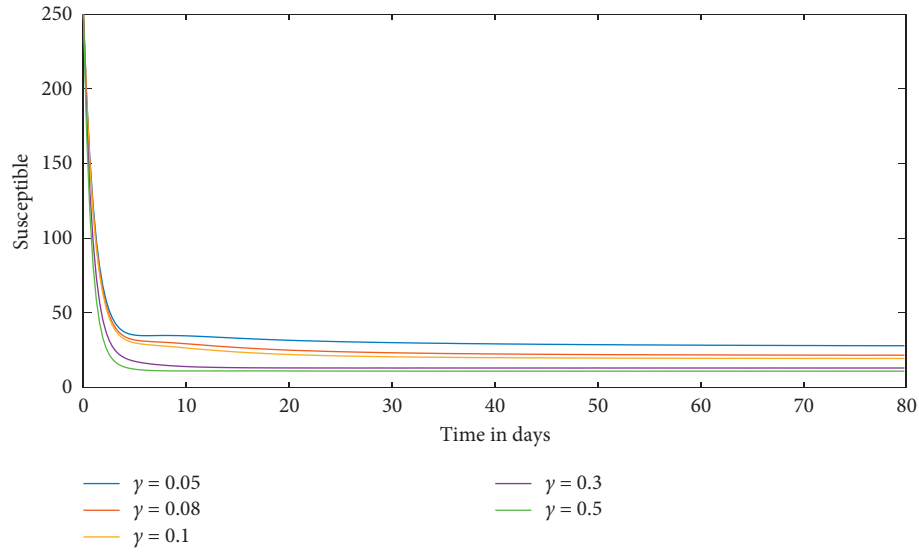

Figure 17: Time series evaluation of susceptible population for $\gamma = 0.05; 0.08; 0.1; 0.3; 0.5$.

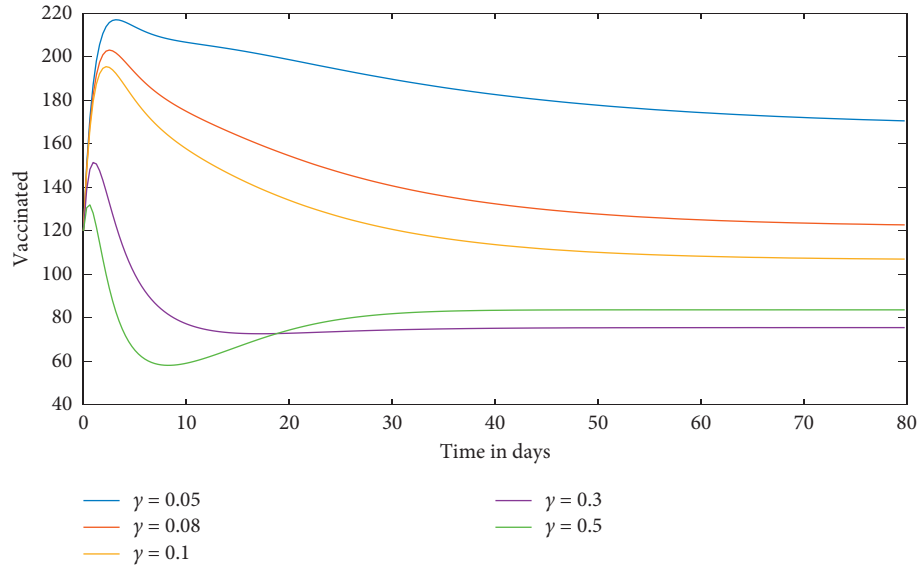

Figure 18: Time series evaluation of vaccinated population for $\gamma = 0.05; 0.08; 0.1; 0.3; 0.5$.

$\beta = 0.05; 0.10; 0.15; 0.20; 0.25$. Figure 10 shows time series evaluation of infected population for $\beta = 0.05; 0.10; 0.15; 0.20; 0.25$. Figure 11 shows time series evaluation of vaccinated population for $\chi = 0.007, 0.009, 0.01, 0.02, 0.03$. Figure 12 shows time series evaluation of infected population $\chi = 0.007, 0.009, 0.01, 0.02, 0.03$. Figure 13 shows time series evaluation of infected population for $\eta = 0.002, 0.006, 0.01, 0.02, 0.03$.

Figure 14 shows time series evaluation of recovered population for $\psi = 0.10, 0.15, 0.20, 0.25, 0.30$. Figure 15 shows time series evaluation of susceptible population for $\Omega = 0.3, 0.5, 0.7$. Figure 16 shows time series evaluation of vaccinated population for $\Omega = 0.3, 0.5, 0.7$. Figure 17 shows time series evaluation of susceptible population for $\gamma = 0.05; 0.08; 0.1; 0.3; 0.5$.

Figure 18 shows time series evaluation of vaccinated population for $\gamma = 0.05; 0.08; 0.1; 0.3; 0.5$. Figure 19 shows time series evaluation of infected population for $\gamma = 0.05; 0.08; 0.1; 0.3; 0.5$. Figure 20 shows time series evaluation of recovered population for $\gamma = 0.05; 0.08; 0.1; 0.3; 0.5$.

Figure 21 shows time series evaluation of susceptible population for $\phi = 0.04; 0.08; 0.2; 0.4; 0.6$. Figure 22 shows time series evaluation of vaccinated population for $\phi = 0.04; 0.08; 0.2; 0.4; 0.6$. Figure 23 shows time series evaluation of recovered population $\phi = 0.04; 0.08; 0.2; 0.4; 0.6$. Figure 24 shows time series evaluation of infected population for $m = 0.5, 3.5, 6.5, 9.5, 12.5$. Figure 25 shows time series evaluation of Recovered population for $m = 0.5, 3.5, 6.5, 9.5, 12.5$. Figure 26 shows time series

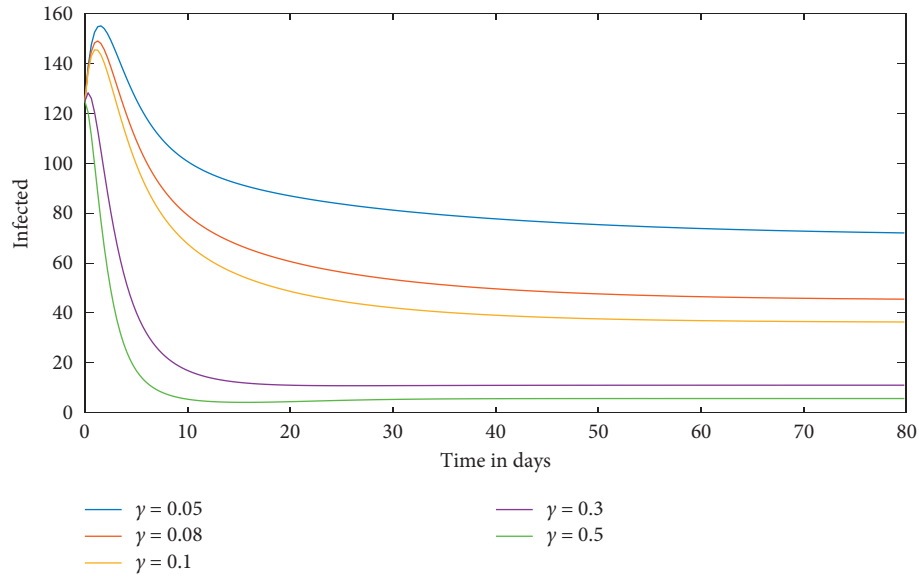

Figure 19: Time series evaluation of infected population for $\gamma = 0.05; 0.08; 0.1; 0.3; 0.5$.

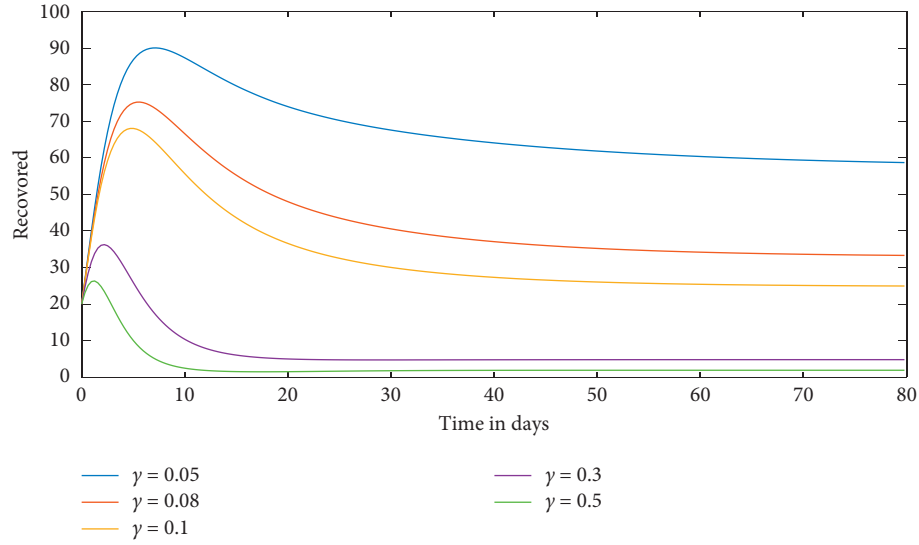

Figure 20: Time series evaluation of recovered population for $\gamma = 0.05; 0.08; 0.1; 0.3; 0.5$.

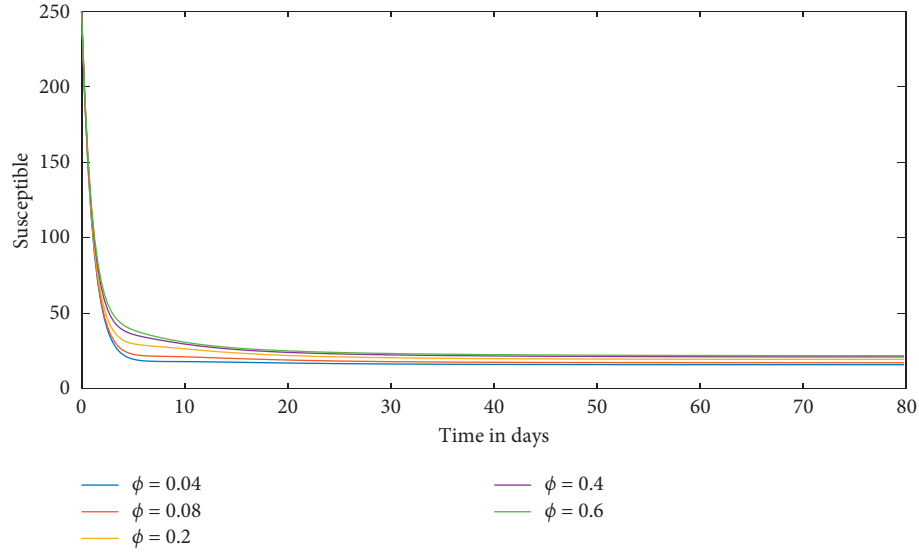

Figure 21: Time series evaluation of susceptible population for $\phi = 0.04; 0.08; 0.2; 0.4; 0.6$.

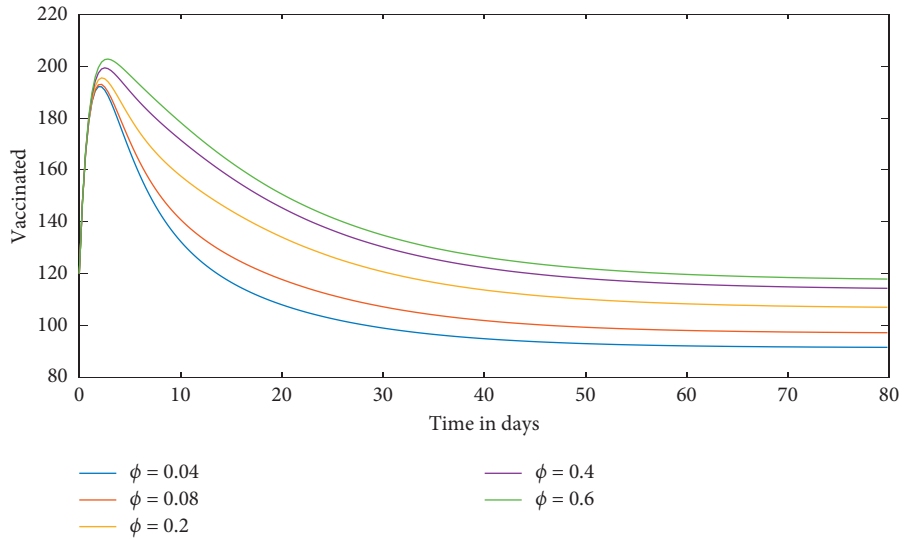

Figure 22: Time series evaluation of vaccinated population for $\phi = 0.04; 0.08; 0.2; 0.4; 0.6$.

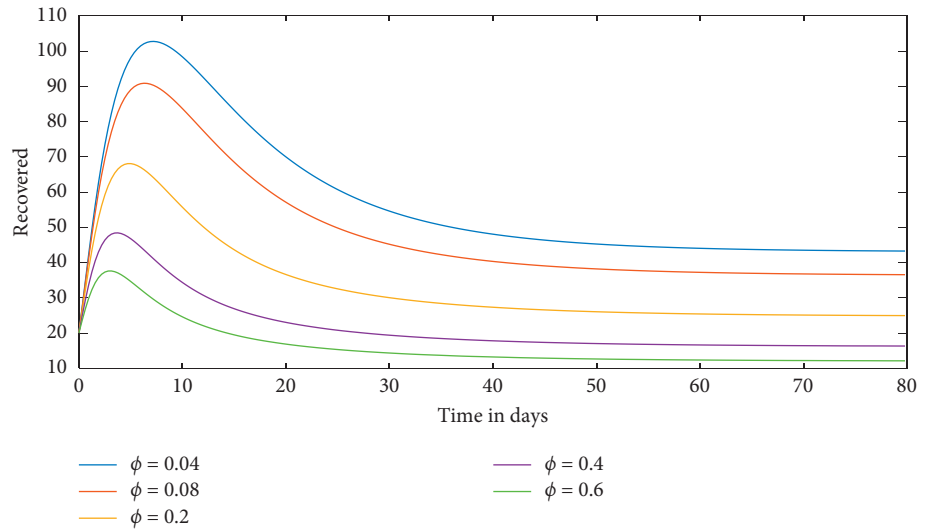

Figure 23: Time series evaluation of recovered population for $\phi = 0.04; 0.08; 0.2; 0.4; 0.6$.

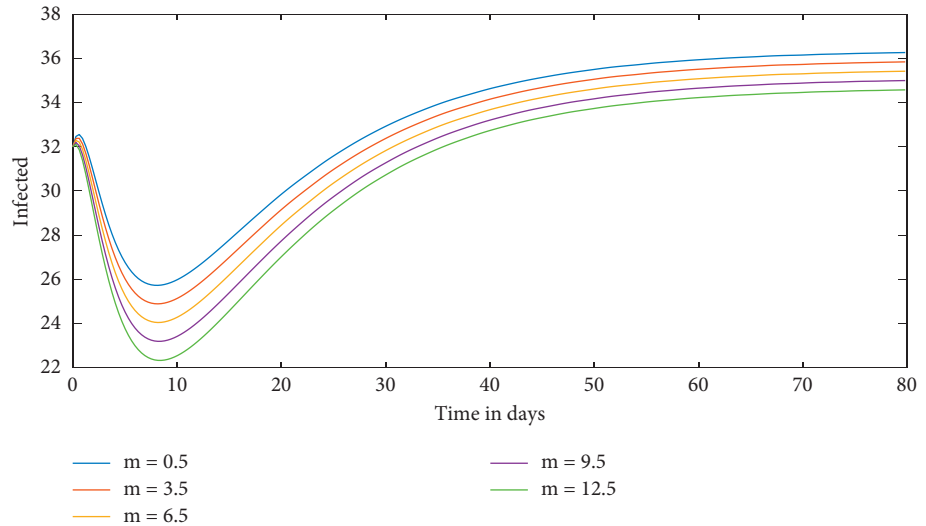

Figure 24: Time series evaluation of infected population for $m = 0.5, 3.5, 6.5, 9.5, 12.5$.

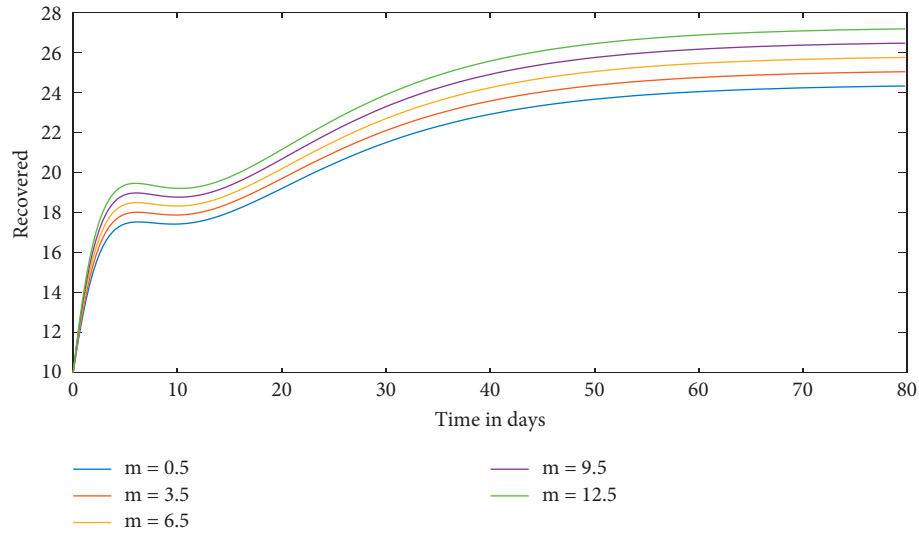

Figure 25: Time series evaluation of recovered population for $m = 0.5, 3.5, 6.5, 9.5, 12.5$.

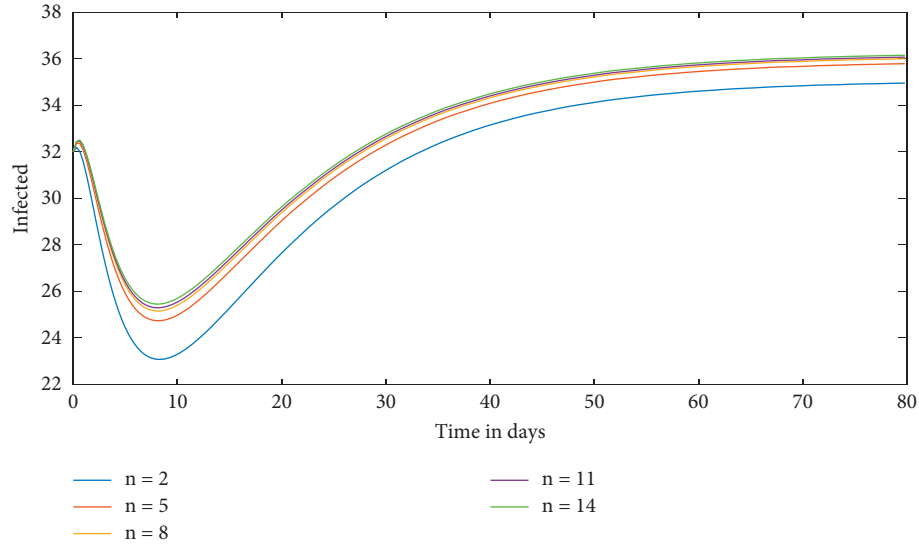

Figure 26: Time series evaluation of recovered population for $n = 2, 5, 8, 10, 14$.

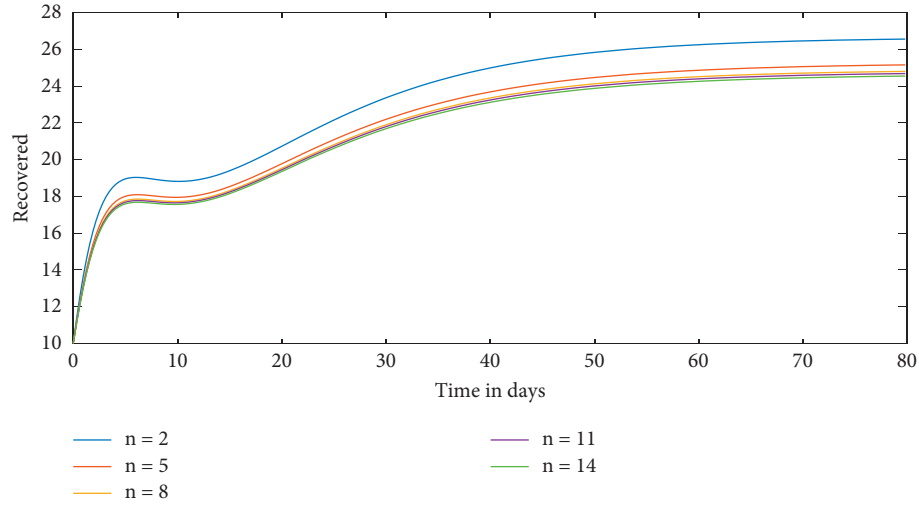

Figure 27: Time series evaluation of recovered population for $n = 2, 5, 8, 10, 14$.

evaluation of recovered population for $n = 2, 5, 8, 10, 14$. Figure 27 shows time series evaluation of recovered population for $n = 2, 5, 8, 10, 14$.

7. Conclusions and Remarks

In this study, we provide a fuzzy SVIRS epidemic model with a Holling type-II incidence rate and saturating treatment, in which all population dynamics parameters are handled as fuzzy integers. The SVIRS model's existence and durability were next investigated, and the disease-free and endemic equilibrium points of the proposed fuzzy system were computed. The Routh–Hurwitz criteria are used to talk about the fuzzy system's local stability conditions around these equilibrium locations. Using the Lozinskii metric, global stability surrounding the internal steady state was also verified. To further understand the dynamics of the suggested model, numerical simulations are provided. The following interpretations are based on the numerical simulations of Section 6:

(i) Figure 4 shows how the population of solution curves (population) changes over time.

(ii) Figure 5 depicts how vulnerable populations change over time at various recruitment rates.

(iii) Figures 6 and 7 show the variations in susceptible and infected populations respectively for various levels of infection force.

(iv) Figures 8, 9, and 10 show how sensitive, vaccinated populations behave over time in days for various inhibitory tactics implemented by the infected. Also, as the sick person's inhibitory measures become more effective, the number of vulnerable and vaccinated people grows. However, as seen in Figure 10, the number of infection individuals is decreasing as the population grows.

(v) The number of people who have been vaccinated has decreased as the values of χ have risen (Figure 11), whereas the number of people who have been infected has increased (Figure 12).

(vi) When the death rate from disease (η) rises, the number of sick people decreases (Figure 13).

(vii) Figure 14 illustrates that the number of recovered individuals grows as the transmission rate from infected persons to recovered individuals (ψ) increases.

(viii) When the transmission rate from susceptible to vaccinated (Ω) is growing, the number of susceptible and vaccinated persons is falling and increasing, respectively (Figures 15 and 16).

(ix) The number of vulnerable (Figure 17), vaccinated (Figure 18), infected (Figure 19), and recovered (Figure 20) persons decreases as the natural death rate (γ) rises.

(x) The number of susceptible (Figure 21) and vaccinated (Figure 22) individuals increases when the transmission rate from recovered individuals to susceptible (ϕ) increases, while the number of recovered individuals (Figure 23) decreases.

(xi) When the treatment rate (m) rises, the number of infected people (Figure 24) falls while the number of recovered people (Figure 25) rises.

(xii) In addition, whenever the rate of medical resource scarcity (m) rises, the number of infected (Figure 26) and recovered (Figure 27) individuals rises and falls, respectively.

(xiii) All parameters play major role in the proposed fuzzy SVIRS, which means the current system can be treated as one of the better solutions for any type of disease models. Previous works focused on stability analysis analytically and numerically, and some are focused on delay dynamics. Delay-induced mathematical model and its analysis also greatly helps us in detecting disease controlling parameters and to detect parameters which allows us to reduce disease transmission.

(xiv) The current work is mainly focused on deterministic (without randomness) approach both analytically and numerically. We can extend this model to capture rich dynamics of system (stochastic model) under noise (randomness, environmental factors around us) by both analytically (using Fourier transform tool) and numerically (using MATLAB software tool). We can extend this model to study the spatio-temporal analysis by constructing a diffusive model using partial differential equations. These can be considered as one of our future projects [51].

Data Availability

The data used to support the findings of this study are included within the article. Should further data or information be required, these are available from the corresponding author upon request.

Conflicts of Interest

The authors declare that there are no conflicts of interest regarding the publication of this paper.

Authors' Contributions

All authors have worked equally. The authors agreed on the used mathematical models, while the first author suggested that the concept of fuzzy parameters should be used to extend the model. The second and third author presented the positivity and boundedness of the system and discussed the stability analysis of the model. The third author presented the numerical simulations of the proposed model.

Acknowledgments

The authors thank Anhui University of Finance and Economics, Bengbu, China, for providing support to complete this research work.

References

[1] W. O. Kermack and A. G. McKendrick, "A contribution to the mathematical theory of epidemics," *Proc R SocLondSer A*, vol. 115, no. 7, pp. 700–721, 1927.

[2] S. Kaliappan, M. D. Raj Kamal, D. S. Mohanamurugan, and D. P. K. Nagarajan, "Analysis of an innovative connecting rod by using finite element method," *Taga Journal of Graphic Technology*, vol. 2018, pp. 1147–1152, 2018.

[3] D. Mukherjee, "Stability analysis of an S-I epidemic model with time delay," *Mathematical and Computer Modelling*, vol. 24, no. 9, pp. 63–68, 1996.

[4] K. Nagarajan, A. Rajagopalan, S. Angalaeswari, L. Natrayan, and W. D. Mammo, "Combined economic emission dispatch of microgrid with the incorporation of renewable energy sources using improved mayfly optimization algorithm," *Computational Intelligence and Neuroscience*, vol. 2022, Article ID 6461690, 22 pages, 2022.

[5] A. d'Onofrio, P. Manfredi, and E. Salinelli, "Vaccinating behaviour, information, and the dynamics of SIR vaccine preventable diseases," *Theoretical Population Biology*, vol. 71, no. 3, pp. 301–317, 2007.

[6] B. Buonomo, A. d'Onofrio, and D. Lacitignola, "Global stability of an SIR epidemic model with information dependent vaccination," *Mathematical Biosciences*, vol. 216, no. 1, pp. 9–16, 2008.

[7] R. H. Martin, "Logarithmic norms and projections applied to linear differential systems," *Journal of Mathematical Analysis and Applications*, vol. 45, no. 2, pp. 432–454, 1974.

[8] K. Goel, "Stability behavior of a nonlinear mathematical epidemic transmission model with time delay," *Nonlinear Dynamics*, vol. 98, no. 2, pp. 1501–1518, 2019.

[9] A. Kumar and K. Goel, "A deterministic time-delayed SIR epidemic model: mathematical modeling and analysis," *Theory in Biosciences*, vol. 139, no. 1, pp. 67–76, 2019.

[10] A. S. Kaliappan, S. Mohanamurugan and P. K. Nagarajan, Numerical investigation of sinusoidal and trapezoidal piston profiles for an IC engine," *Journal of Applied Fluid Mechanics*, vol. 13, no. 1, pp. 287–298, 2020.

[11] A. Kumar, "Stability of a delayed SIR epidemic model by introducing two explicit treatment classes along with nonlinear incidence rate and Holling type treatment," *Computational and Applied Mathematics*, vol. 38, no. 3, p. 130, 2019.

[12] D. K. Jain, S. K. S. Tyagi, S. Neelakandan, M. Prakash, and L. Natrayan, "Metaheuristic optimization-based resource allocation technique for cybertwin-driven 6G on IoE environment," *IEEE Transactions on Industrial Informatics*, vol. 18, no. 7, pp. 4884–4892, 2022.

[13] B. Dubey, A. Patra, P. K. Srivastava, and U. S. Dubey, "Modeling and analysis of an SEIR model with different types of nonlinear treatment rates," *Journal of Biological Systems*, vol. 21, no. 03, Article ID 1350023, 2013.

[14] S. Tipsri and W. Chinviriyasit, "Stability analysis of SEIR model with saturated incidence and time delay," *International Journal of Applied Physics and Mathematics*, vol. 4, no. 1, pp. 42–45, 2014.

[15] A. B. Gumel, C. C. McCluskey, and J. Watmough, "An SVEIR model for assessing potential impact of an imperfect anti-sars vaccine," *Mathematical Biosciences and Engineering*, vol. 3, no. 3, pp. 485–512, 2006.

[16] K. R. Vaishali, S. R. Rammohan, L. Natrayan, D. Usha, and V. R. Niveditha, "Guided container selection for data streaming through neural learning in cloud," *International Journal of System Assurance Engineering and Management*, vol. 16, pp. 1–7, 2021.

[17] A. Darshan, N. Girdhar, R. Bhojwani et al., "Energy audit of a residential building to reduce energy cost and carbon footprint for sustainable development with renewable energy sources," *Advances in Civil Engineering*, vol. 2022, pp. 1–10, Article ID 4400874, 2022.

[18] P. Asha, L. Natrayan, B. Geetha et al., "IoT enabled environmental toxicology for air pollution monitoring using AI techniques," *Environmental Research*, vol. 205, Article ID 112574, 2022.

[19] S. S. Sundaram, N. H. Basker, and L. Natrayan, "Smart clothes with bio-sensors for ECG monitoring," *International Journal of Innovative Technology and Exploring Engineering*, vol. 8, no. 4, pp. 298–301, 2019.

[20] F. Brauer, "Backward bifurcations in simple vaccination models," *Journal of Mathematical Analysis and Applications*, vol. 298, no. 2, pp. 418–431, 2004.

[21] C. N. Podder and A. B. Gumel, "Qualitative dynamics of a vaccination model for HSV-2," *IMA Journal of Applied Mathematics*, vol. 75, no. 1, pp. 75–107, 2010.

[22] O. Sharomi, C. N. Podder, A. B. Gumel, S. M. Mahmud, and E. Rubinstein, "Modelling the transmission dynamics and control of the Novel 2009 swine influenza (H1N1) pandemic," *Bulletin of Mathematical Biology*, vol. 73, no. 3, pp. 515–548, 2011.

[23] A. B. Gumel, "Causes of backward bifurcations in some epidemiological models," *Journal of Mathematical Analysis and Applications*, vol. 395, no. 1, pp. 355–365, 2012.

[24] M. Safan and F. A. Rihan, "Mathematical analysis of an SIS model with imperfect vaccination and backward bifurcation," *Mathematics and Computers in Simulation*, vol. 96, pp. 195–206, 2014.

[25] A. d'Onofrio and P. Manfredi, "Bistable endemic states in a susceptible-infectious-susceptible model with behavior-dependent vaccination," in *Proceedings of the Mathematical and Statistical Modeling for Emerging and Re-emerging Infectious Diseases*, G. Chowell and J. Hyman, Eds., Springer, Cham, pp. 341–354, July 2016.

[26] C. S. S. Anupama, L. Natrayan, E. Laxmi Lydia et al., "Deep learning with backtracking search optimization based skin lesion diagnosis model," *Computers, Materials & Continua*, vol. 70, no. 1, pp. 1297–1313, 2021.

[27] A. d'Onofrio and P. Manfredi, "Information-related changes in contact patterns may trigger oscillations in the endemic prevalence of infectious diseases," *Journal of Theoretical Biology*, vol. 256, no. 3, pp. 473–478, 2009.

[28] R. M. Anderson and R. M. May, "Regulation and stability of host–parasite population. Interactions: I. Regulatory processes," *Journal of Animal Ecology*, vol. 47, no. 1, pp. 219–267, 1978.

[29] C. Wei and L. Chen, "A delayed epidemic model with pulse vaccination," *DiscretDyn Nat Soc*, vol. 2008, Article ID 746951, 12 pages, 2008.

[30] J. Z. Zhang, Z. Jin, Q. X. Liu, and Z. Y. Zhang, "Analysis of a delayed SIR model with nonlinear incidence rate," *DiscretDyn Nat Soc*, vol. 2008, Article ID 636153, 12 pages, 2008.

[31] X. Z. Li, W. S. Li, and M. Ghosh, "Stability and bifurcation of an SIR epidemic model with nonlinear incidence and treatment," *Applied Mathematics and Computation*, vol. 210, no. 1, pp. 141–150, 2009.

[32] A. Kumar, "Stability of a time delayed SIR epidemic model along with nonlinear incidence rate and Holling type-II

treatment rate," *International Journal of Computational Methods*, vol. 15, no. 06, Article ID 1850055, 2018.

[33] A. Kumar, "Dynamical model of epidemic along with time delay; Holling type II incidence rate and Monod-Haldane type treatment rate," *Differ EquDynSyst*, vol. 27, no. 1–3, pp. 299–312, 2018.

[34] A. Kumar, "Mathematical analysis of a delayed epidemic model with nonlinear incidence and treatment rates," *Journal of Engineering Mathematics*, vol. 115, no. 1, pp. 1–20, 2019.

[35] K. Goel, "A mathematical and numerical study of a SIR epidemic model with time delay, nonlinear incidence and treatment rates," *Theory in Biosciences*, vol. 138, no. 2, pp. 203–213, 2019.

[36] L. Zhou and M. Fan, "Dynamics of an SIR epidemic model with limited medical resources revisited," *Nonlinear Analysis: Real World Applications*, vol. 13, no. 1, pp. 312–324, 2012.

[37] M. Yang and F. Sun, "Global stability of SIR models with nonlinear Incidence and discontinuous treatment," *The Electronic Journal of Differential Equations*, vol. 2015, no. 304, pp. 1–8, 2015.

[38] K. Goel and A. Kumar, "A deterministic time-delayed SVIRS epidemic model with incidences and saturated treatment," *Journal of Engineering Mathematics*, vol. 121, no. 1, pp. 19–38, 2020.

[39] X. B. Liu and L. J. Yang, "Stability analysis of an SEIQV epidemic model with saturated incidence rate," *Nonlinear Analysis: Real World Applications*, vol. 13, no. 6, pp. 2671–2679, 2012.

[40] S. Magesh, V. R. Niveditha, P. S. Rajakumar, and L. Natrayan, "Pervasive computing in the context of COVID-19 prediction with AI-based algorithms," *International Journal of Pervasive Computing and Communications*, vol. 16, no. 5, pp. 477–487, 2020.

[41] O. A. Arqub, A. Elajou, S. Momani, and N. Shawagfeh, "Analytical Solutions of fuzzy initial value problem by HAM," *Appl.Math.Inform.Sci*, vol. 7, pp. 1903–1919, 2013.

[42] O. A. Arqub, "series solution of a fuzzy differential equation under strongly generalized differentiability," *J.Adv.Res.Appl.Math*, vol. 5, pp. 31–52, 2013.

[43] P. K. Mondal, S. Jana, P. Haldar, and T. K. Kar, "Dynamical behavior of an epidemic model in a fuzzy transmission," *Int.J.Unc.Fuzz.Knowl.BasedSyst.*vol. 23, no. 05, pp. 651–665, 2015.

[44] D. Nagarajan, M. Lathamaheswari, S. Broumi, and J. Kavikumar, "A new perspective on traffic control management using triangular interval type-2 fuzzy sets and interval neutrosophic sets," *Operations Research Perspectives*, vol. 6, Article ID 100099, 2019.

[45] A. sendrayaperumal, S. Mahapatra, S. S. Parida et al., "Energy auditing for efficient planning and implementation in commercial and residential buildings," *Advances in Civil Engineering*, vol. 2021, Article ID 1908568, 10 pages, 2021.

[46] L. C. Barros, M. Leite, and R. Bassanezi, "The SI epidemiological models with a fuzzy transmission parameter," *Computers & Mathematics with Applications*, vol. 45, no. 10-11, pp. 1619–1628, 2003.

[47] L. P. Natrayan, "Sakthi shunmuga sundaram. J. Elumalai. Analyzing the Uterine physiological with MMG Signals using SVM," *International journal of Pharmaceutical research*, vol. 11, no. 2, pp. 165–170, 2019.

[48] G. J. Klir and B. Yuan, "Fuzzy sets and fuzzy logic: theory and applications. Possibility Theory versus Probab," *Theory*, vol. 32, no. 2, pp. 207-208, 1996.

[49] S. Adak and S. Jana, "Dynamical behavior of an epidemic model with fuzzy transmission and fuzzy treatment control," *J. Appl. Math. Comput.*vol. 68, no. 3, pp. 1929–1948, 2021.

[50] S. K. Nandi, S. Jana, M. Manadal, and T. K. Kar, "Analysis of a fuzzy epidemic model with saturated treatment and disease transmission," *International Journal of Biomathematics*, vol. 11, no. 01, Article ID 1850002, 2018.

[51] Y. T. Mangongo, J. D. K. Bukweli, and J. D. B. Kampempe, "Fuzzy global stability analysis of the dynamics of malaria with fuzzy transmission and recovery rates," *American Journal of Operations Research*, vol. 11, no. 06, pp. 257–282, 2021.

[52] M. K. Sharma, N. Dhiman, N. Vandana, and V. N. Mishra, "Mediative fuzzy logic mathematical model: a contradictory management prediction in COVID-19 pandemic," *Applied Soft Computing*, vol. 105, Article ID 107285, 2021.

[53] N. Lefevr, A. Kanavos, V. C. Gerogiannis, L. Iliadis, and P. Pintelas, "Employing fuzzy logic to analyze the structure of complex biological and epidemic spreading models," *Mathematics*, vol. 9, p. 977, 2021.

[54] J. Zhang, J. Jia, and X. Song, "Analysis of an SEIR epidemic model with saturated incidence and saturated treatment function," *The Scientific World Journal*, vol. 2014, Article ID 910421, 11 pages, 2014.